

DRL No. 206
DRD No. SE-6
Item #6

WAESD-TR-86-0015
DOE/JPL-956616-86/1
Distribution Category UC-63

IN - CAT. 44

72103 - R

82P

FLAT-PLATE SOLAR ARRAY PROJECT
PROCESS DEVELOPMENT AREA
PROCESS RESEARCH OF NON-CZ SILICON MATERIAL

FINAL REPORT

November, 1983 to January, 1986

CONTRACT NO. 956616
956616 - Mod 1
956616 - Mod 2

The JPL Flat-Plate Solar Array Project is sponsored by the U.S. Department of Energy and forms part of the Solar Photovoltaic Conversion Program to initiate a major effort toward the development of low-cost solar arrays. This work was performed for the Jet Propulsion Laboratory, California Institute of Technology, by agreement between NASA and DOE.

(NASA-CR-180607) FLAT-PLATE SOLAR ARRAY
PROJECT PROCESS DEVELOPMENT AREA: PROCESS
RESEARCH OF NON-CZ SILICON MATERIAL Final
Report, Nov. 1983 - Jan. 1986 (Westinghouse
Electric Corp.) 82 p Avail: NTIS HC

N87-22302

Unclas
G3/44 0072103

Advanced Energy Systems Division
WESTINGHOUSE ELECTRIC CORPORATION
P. O. Box 10864
Pittsburgh, PA 15236-0864

FLAT-PLATE SOLAR ARRAY PROJECT
PROCESS DEVELOPMENT AREA

PROCESS RESEARCH OF NON-CZ SILICON MATERIAL

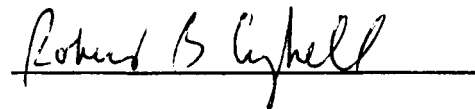
FINAL REPORT
November 1983 - January 1986

Contract No. 956616
956616 - Mod 1
956616 - Mod 2

The JPL Flat-Plate Solar Array Project is sponsored by the U.S. Department of Energy and forms part of the Solar Photovoltaic Conversion Program to initiate a major effort toward the development of low-cost solar arrays. This work was performed for the Jet Propulsion Laboratory, California Institute of Technology, by agreement between NASA and DOE.

Prepared by:

Approved by



R. B. Campbell
Principal Investigator



C. M. Rose
Project Manager

Advanced Energy Systems Division
WESTINGHOUSE ELECTRIC CORPORATION
P. O. Box 10864
Pittsburgh, PA 15236-0864

TECHNICAL CONTENT STATEMENT

"This report was prepared as an account of work sponsored by the United States Government. Neither the United States nor the United States Department of Energy, nor any of their employees, nor any of their contractors, subcontractors, or their employees makes any warranty, expressed or implied, or assumes any legal liability or responsibility for the accuracy, completeness or usefulness of any information, apparatus, product or process disclosed, or represented that its use would not infringe privately owned rights."

TABLE OF CONTENTS

	<u>Page</u>
1.0 INTRODUCTION	1
2.0 TECHNICAL PROGRESS	4
2.1 Background	4
2.2 Simultaneous Diffusion Standard Time/Temperature Cycle	5
2.2.1 Conditions for Stain Free Surfaces After Diffusion	5
2.2.2 Diffusion Experiments	7
2.2.3 Later Approaches	15
2.2.4 Sequential Diffusion of N-Type Web	20
2.2.5 Simultaneous Diffusion Using a Belt Furnace	21
2.2.6 Conclusions - Simultaneous Diffusions Standard Time/Temperature Cycle	24
2.3 Laser Drive-In for Simultaneous Diffusion	24
2.3.1 Background	24
2.3.2 Experimental Results, Initial Test	24
2.3.3 Subsequent Laser Drive Experimental Results	33
2.3.4 Conclusions	41
2.4 Junction Formation by Pulsed Directed Heating (Flash Diffusion)	43
2.4.1 Introduction	43
2.4.2 Experimental Results	45
2.4.3 Conclusions	62
3.0 COST ANALYSIS	63
4.0 CONCLUSIONS	73

LIST OF TABLES

<u>Table No.</u>	<u>Title</u>	<u>Page</u>
1	Diffusion Conditions for Front Junction - N-Type Web	6
2	Process Sequence for Simultaneous Diffusion of N-Type Web	8
3	Simultaneous Diffusion Experiments and Results	12
4	Simultaneous Diffusion Experiments Conducted with Diffusion Masks Applied by Dip Coating	16
5	Low Temperature, Arsenic and P-Type Web Simultaneous Diffusion Experiment Summaries	18
6	Sequential Diffusion of N-Type Web	22
7	Laser Drive In Diffusion Test	26
8	Data from Cells Fabricated Using an Excimer Laser to Form the Junctions	31
9	Cell Properties Measured After Heat Treatment of Laser Processed Cells	32
10	Range Parameters - Laser Drive In Tests	34
11	Lighted IV Parameters of Representative Laser Processed Samples	38
12	Dark IV Data From Selected Laser Processed Cells	39
13	Lighted and Dark IV Data From Laser Processed Cells After Annealing and Back Surface Damage	40
14	Dark IV Data From Further Laser Processed Cells	42
15	Results of Conductivity and Sheet Resistivity Measurements Made on Flash Diffused Junctions	46
16	Lighted IV Dark - Cells Fabricated on Web with Junctions Formed by Pulsed Directed Heating	52
17	Dark IV Data - Cells Fabricated on Web with Junctions Formed by Flash Diffusion	53
18	Flash Diffusion Verification Experiment Outline	55
19	Flash Diffusion Verification Experiment	56
20	Diffusion Length Measurements on Selected Flash Diffused Cells	58

LIST OF TABLES (Continued)

<u>Table No.</u>	<u>Title</u>	<u>Page</u>
21	Collected Data from Flash Diffused Cells	61
22	Format A - 1 MW/yr	64
23	Format A - 1 MW/yr	65
24	Format A - 25 MW/yr	67
25	Format A - 25 MW/yr	68
26	Cost Factors - 1 MW/Yr and 25 MW/Yr Facilities	71
27	Cost of Flash Diffusion vs. Sequential Diffusion	72

LIST OF FIGURES

<u>Figure No.</u>	<u>Title</u>	<u>Page</u>
1	P ⁺ N Front Junction Profile Measured on Simultaneously Diffused Web Strip #49125-21A	10
2	N ⁺ N Back Junction Profile Measured on Simultaneously Diffused Web Strip #49125-21A	11
3	Photomicrographs of Sample 17B Surfaces After Laser Drive of Phosphorus and Boron	27
4	N ⁺ P Front Junction Profile Measured After Laser Drive on Sample 49B	28
5	P ⁺ P Back Junction Profile Measured After Laser Drive on Sample 49B	29
6	Spreading Resistance Profiles of N ⁺ P Junction Taken 1.5 mm Apart	36
7	Typical Heating Cycle for Short Time-High Temperature Diffusion	44
8	Front N ⁺ P Junction Formed by Short Time-High Temperature Diffusion	47
9	Back P ⁺ P Junction Formed by Short Time-High Temperature Diffusion	48
10	P ⁺ N Front Junction	49
11	N ⁺ N Back Junction	50
12	Cell Efficiency vs Annealing Cycle N Base and P Base Cells	59
13	Quantum Efficiency of an N Base Cell and a P Base Cell	60

1.0 INTRODUCTION

This final report discusses results of studies on Contract 956616 and Modifications 1 and 2 of this contract entitled "Process Research of Non-Cz Silicon Material."

The major objectives of this program were:

- Develop a process for simultaneously diffusing the front and back junctions into dendritic web silicon to form a solar cell structure.
- Determine process control parameters and the sensitivity of cell parameters to variations in these control parameters.
- Perform a cost analysis on the simultaneous junction formation method and compare this result to a sequential diffusion process.

All of the studies mentioned above were carried out on dendritic web silicon grown on the Westinghouse Pre-Pilot facility. Dendritic web is a ribbon form of single crystal sheet material produced (grown) from a molten silicon charge using a dendritic seed. The web can be grown as either N-type or P-type conductivity with a wide range resistivity levels. Conductivity and resistivity levels are controlled by the dopants added to the molten silicon during the growth cycle. Dendritic web is a high quality, pure, crystalline material and cells have been fabricated on web with efficiencies in excess of 15% using a standard process sequence developed by Westinghouse. The standard sequence uses a sequential diffusion process for front and back junction formations. Thus cell data obtained in the simultaneous diffusion experiments conducted in this contract can be correlated with cells produced using the baseline sequence.

During the program three basic techniques were used to study simultaneous junction formation in dendritic web silicon. The first was a diffusion where phosphorous and boron containing liquid metallorganic precursors* were applied to the appropriate sides of a strip of dendritic web silicon, dried and

*Hereafter, these liquids will be referred to as liquid dopants.

diffused at standard temperature/time cycles in a tube type diffusion furnace or a belt furnace. Due to the diffusion constants of boron and phosphorous these tests were carried out on N-type dendritic web to achieve the proper front and back junction depths. The proper junction depths were achieved but in nearly all cases, the phosphorous diffusant contaminated the boron doped junction causing diffusion spikes, and cells with a very low efficiency. Various types of SiO_2 masks were studied in an attempt to prevent this cross doping without success. In a parallel effort the diffusion was carried out in a belt furnace. In general the results were the same.

The second method used was to drive the liquid dopants into the web surface using an excimer laser. In these tests the dopants on the two sides were driven in sequentially; however it was recognized that with suitable engineering of two laser heads, the drive in could be accomplished simultaneously. In this series of experiments, high quality junctions were obtained with phosphorous doping; however only very shallow junctions were achieved with the boron doping. With these shallow junctions low resistance contacts to the back surface were not obtained, and the cells had efficiencies in the 8-12% range.

The third technique investigated for simultaneous junction formation used rapid thermal processing equipment. In these tests the web strips, coated with the dopants were subjected to a high temperature - short term heat pulse from high intensity tungsten-halogen flash lamps. Nominal values of time and temperature used were 10 sec and 1100°C. In these tests, excellent cells were obtained on N-type material with efficiencies exceeding 15%.

There are several distinct advantages to the rapid thermal pulse junction formation. First the junction formation is rapid, taking less than 1% of the normal time. This reduces both processing time and energy costs. Second, since junction formation occurs rapidly, cross-contamination of the dopants does not occur. Finally since the procedure forms the junctions simultaneously, the processing time is further reduced since one less cleaning and etching step is required in the cell processing sequence. Although efficiencies greater than 15% were obtained with N-type material, cells from P-base material treated in the same way gave lower efficiencies.

To achieve the highest cell efficiencies an annealing cycle is required after the initial diffusion process to remove quenched in defects due to rapid cooling. During the program an optimum annealing time/temperature matrix were determined. The temperature and time chosen are such that no re-distribution of the dopant species takes place during the cycle.

A cost analysis was performed on this third method for simultaneous junction formation and the results indicate greater than a 60% saving (for this step) in a large scale automated production line.

2.0 TECHNICAL PROGRESS

2.1 Background

In this section, the results of three different simultaneous diffusion techniques will be discussed. All of these studies were carried out using dendritic web silicon grown on the Westinghouse pre-pilot facility.

In the baseline sequence developed by Westinghouse, P-type dendritic web is processed into solar cells by a sequential process in which the boron doped P^+P back junction with a junction depth of $0.5 \pm 0.1 \mu\text{m}$ is prepared first followed by the phosphorous doped N^+P front junction with a junction depth of $0.25 \pm 0.3 \mu\text{m}$. Since phosphorous diffuses at a faster rate than boron, the diffusion for the front junction is made at about 100°C lower temperature.

In a simultaneous diffusion process where both junctions are formed at the same temperature, the phosphorous doped junctions will be much deeper due to the larger diffusion constant. Thus a $N^+P P^+$ cell structure would have a significantly deeper front junction than required.

One method obviating this problem is to use N-base web and form an $P^+N N^+$ cell structure. In this case, the front (boron doped) junction could be controlled to the proper depth and the back (phosphorous doped) junction would be considerably deeper as required for a back surface field. Therefore most of the experiments discussed here were carried out on N-type web.

The dopant sources used in all experiments were liquid metallorganic precursors containing phosphorus, boron or other P-type or N-type dopants under study. These dopants were painted on the appropriate surface of the web, dried and baked to remove all excess solvent. The normal drying temperature was 90°C for 10 min in air followed by baking at 200°C in air for 20 minutes. At the end of this treatment the sources formed a hard, adherent glass-like coating. After the diffusion experiment, the residual glasses were removed by etching in dilute HF.

2.2 Simultaneous Diffusion Standard Time/Temperature Cycle

2.2.1 Conditions for Stain Free Surfaces After Diffusion

In a previous Westinghouse program (JPL Contract 955909), a boron back surface field was prepared using a liquid boron compound as the diffusion source for the back junction. In those studies, it was noted that there was residual staining of the back surface due to incomplete removal of the boron glass after diffusion. That stain, believed to be a silicon-nitrogen compound, could not be removed using the normal HF-H₂O stripping solution.

Experimental data indicated that those stains did not adversely affect the cell parameters in these N⁺PP⁺ cells. However, stains on the front (sun) side of the cell will degrade cell performance since the antireflective solution coats non-uniformly over the stain.

Thus, the first several processing experiments were carried out to determine conditions where the stain would not occur.

Table 1 gives a summary of conditions used for these tests. The B-150 dopant was diluted with toluene in several runs based on data from previous work where the staining was less pronounced with a diluted dopant. The web strips which had sheet resistivities in the 40-50 Ω/\square range (Rows 1 and 5 in Table 1) had junction depths of 0.3 to 0.4 μm . This is slightly deeper than desired for a front junction, but can be readily adjusted by varying the diffusion times and temperatures.

These data, which show higher sheet resistivities when using oxygen in the ambient gas, are similar to results obtained in earlier work⁽¹⁾⁽²⁾. The referenced papers suggest that as the oxygen concentration is increased, thermal oxidation of the dopant competes with the diffusion process; and there is less dopant available for diffusion and therefore a shallower junction depth.

TABLE 1
DIFFUSION CONDITIONS FOR FRONT JUNCTION - N-TYPE WEB⁽¹⁾

<u>Diffusion Temp. (°C)</u>	<u>Diffusion Time (min.)</u>	<u>Gas Flow and Composition</u>	<u>Sheet Res. (Ω/\square)</u>	<u>Dopant</u>	<u>Stripping Solution</u>	<u>Comments</u>
980	20	1000 cc/min N ₂	40-50	B-150	1/10-HF/H ₂ O Cold	Stained
980	20	750 cc/min N ₂ +750 cc/min O ₂	100-1000	DIL B-150 ⁽²⁾	1/10-HF/H ₂ O Hot	Slight stains
980	20	750 cc/min N ₂ +750 cc/min O ₂	100-1000	DIL B-150 ⁽²⁾	1/10-HF/H ₂ O Cold	No stains
980	20	750 cc/min O ₂	200-2000	DIL B-150 ⁽²⁾	1/10-HF/H ₂ O Cold	Slight staining
980	20	750 cc/min N ₂	40-50	<u>DIL B-150⁽²⁾</u>	1/10-HF/H ₂ O Cold	No stains

(1) Web Used - Run 1.208 (0.7 Ω -cm)

(2) B-150 diluted 50% with toluene (B-150 is a tradename of a boron dopant prepared by Allied Chemical Co.).

From these tests, it is concluded that when using the B-150 dopant, optimal results are obtained using nitrogen as the ambient gas and a diluted dopant (e.g., B-150 diluted 50% with toluene).

Since the object of the work was to simultaneously form junctions, tests were carried out using a liquid phosphorous dopant source (PX-10; Allied Chemical). The diffusion conditions were the same as those given in Table 1. Sheet resistivities of 10-30 Ω/\square and with junction depths of 0.8 μm were obtained. Thus, it was determined that the back junction (N^+N) can be prepared under the same diffusion conditions as the front P^+N junction.

The initial tests showed that: 1) a stain free front surface could be obtained, and 2) proper front and back junction depths could be obtained with N-type web using a single set of diffusion conditions.

2.2.2 Diffusion Experiments

The process sequence used in this program to simultaneously diffuse back and front junction in N-type web is shown in Table 2. All previous and subsequent steps in the cell process sequence were identical to those of the baseline Westinghouse process for producing N^+PP^+ cells.

Initial tests investigated diffusion conditions listed in Step 5 of Table 2. Proper front and back junction depths were achieved with diffusion temperatures ranging from 940 to 960°C, diffusion times ranging from 18 to 25 minutes, and with a 1000 cc/min gas ambient of N_2 . In some tests, the final 5 minutes were carried out in 500 cc/min of O_2 .

These diffusion conditions produced front junction depths of 0.2 - 0.3 μm and back junction depths of 0.4 - 0.8 μm as determined by spreading resistivity measurements.

TABLE 2
PROCESS SEQUENCE FOR SIMULTANEOUS DIFFUSION OF N-TYPE WEB

1. Using a P-type liquid organometallic precursor, paint dopant on defined front surface of pre-cleaned web.
2. Dry and bake per vendor instructions.
3. Using a N-type liquid organometallic precursor, paint dopant on defined back side of web.
4. Dry and bake per vendor instructions.
5. Diffuse at predetermined temperature, time, and gas ambients.

Front and rear junction profiles for a representative dendritic web cell which was simultaneously diffused are shown in Figures 1 and 2, respectively.

Figure 1 shows the front P^+N junction with a junction depth of $0.2\text{ }\mu\text{m}$ and a surface concentration near $10^{20}/\text{cm}^3$. The slight curvature at the beginning of the curve indicates a "starved" source, i.e., there were not sufficient phosphorus atoms in the source to prevent depletion at the surface during the drive process.

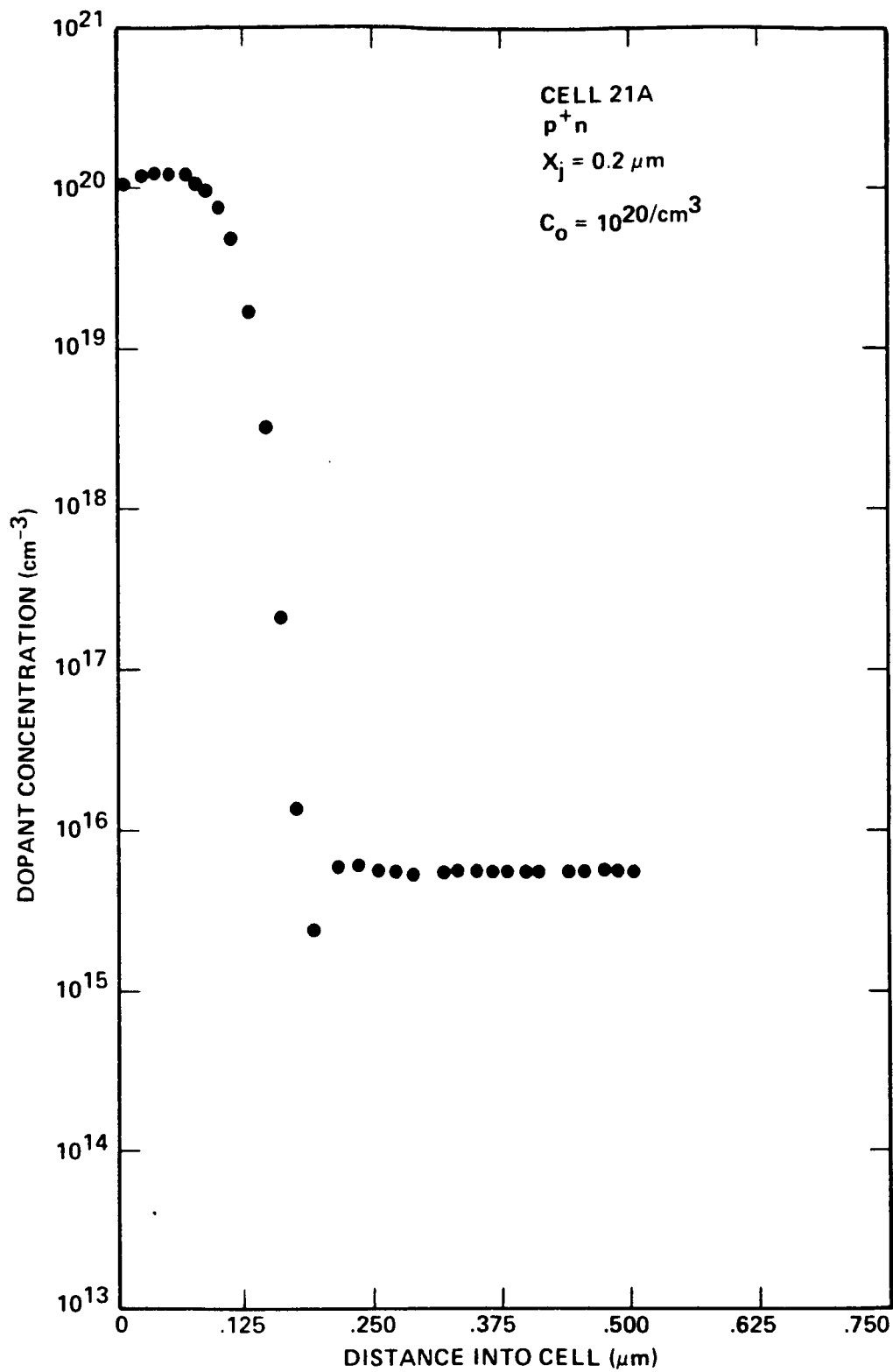
Figure 2 shows the back N^+N junction for the same cell. Here the junction depth is $0.8\text{ }\mu\text{m}$ with a surface concentration of about $2 \times 10^{20}/\text{cm}^3$. Again, the effect of the "starved" source is seen.

These figures indicate that proper diffusion conditions have been obtained to achieve a P^+NN^+ cell by simultaneous diffusion.

When strips diffused under these conditions were processed into finished cells, very low efficiencies (on the order of 1-5%) were obtained. The strips were carefully checked with a conductivity probe, and while the back surface was totally N-type there were small areas of N-type material on the P-type front surface. That is, the front surface was contaminated with phosphorous dopant, causing diffusion spikes and electrical shorts in the P^+N junction. Extreme care was taken in the dopant application to prevent any phosphorous getting on the front surface, which leads to the conclusion that the contamination occurred during the diffusion.

In the next series of experiments, the surfaces of the web were coated with an undoped SiO_2 glass (after the dopant application) to inhibit or control this contamination (or cross-doping). Table 3 lists the diffusion conditions and the results obtained in a number of experiments which included the SiO_2 mask.

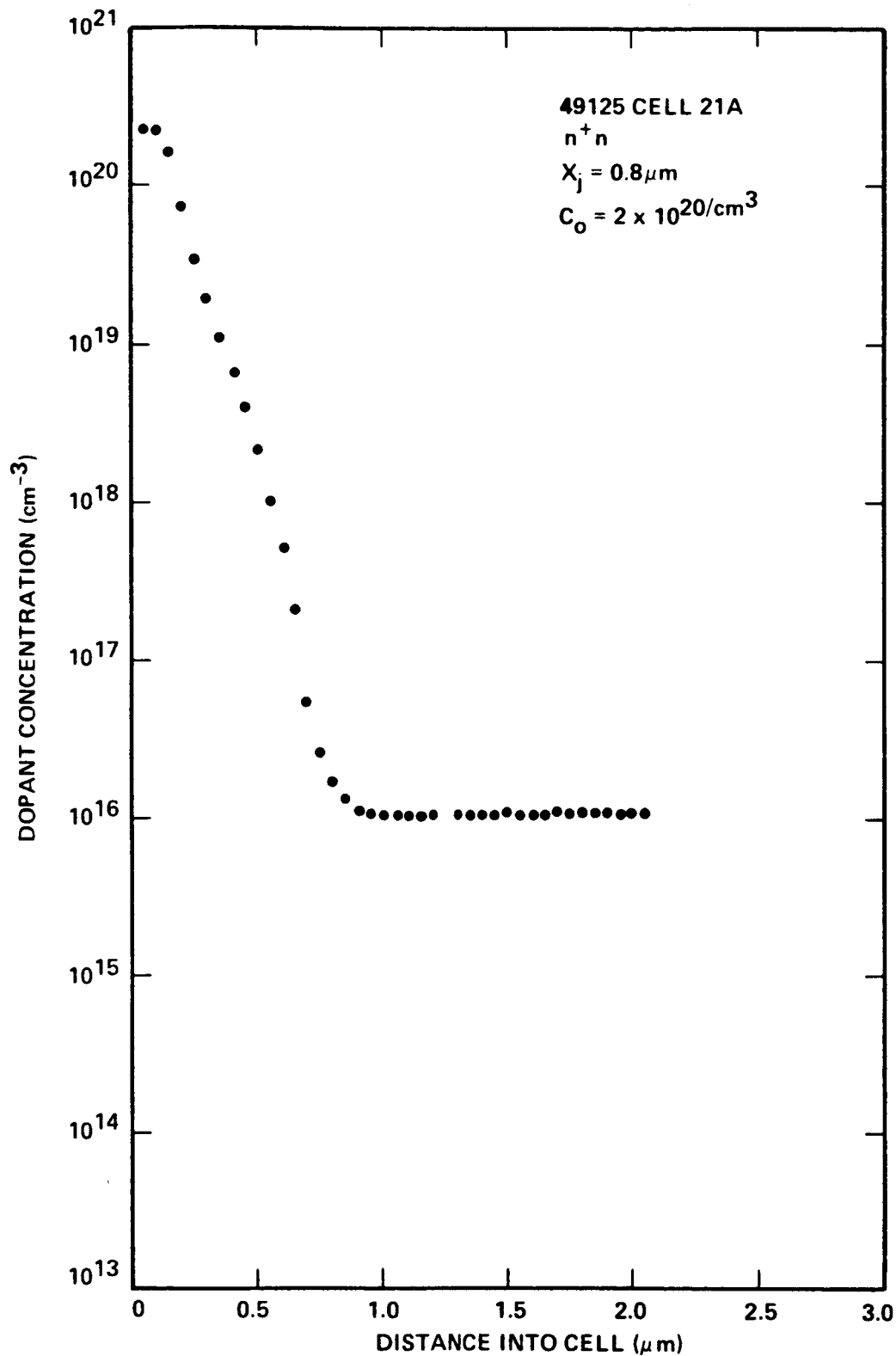
Several different SiO_2 glasses were used in these tests. U1A is used as a diffusion mask in the baseline process for N^+PP cells. X600 and NP-5R are experimental SiO_2 solutions obtained from Allied Chemical Corporation and require baking at higher temperatures to achieve a hard glass.



PV860402-6

Figure 1. P⁺N Front Junction Profile Measured on Simultaneously Diffused Web Strip #49125-21A

05840:3



PV860402-5

Figure 2. N^+N Back Junction Profile Measured on Simultaneously Diffused Web Strip #49125-21A

TABLE 3
SIMULTANEOUS DIFFUSION EXPERIMENTS AND RESULTS

Run ID	P ⁺ Dopant	N ⁺ Dopant	Diffusion Conditions	Sheet Resistivity (Ω/\square)		Cell Data (Efficiency)	Comments
				P ⁺	N ⁺		
49133	B150	PX10	960°C/20 min	1K	8-10	No PN Junction	B150 masked with UIA (SiO ₂)
49137	Dil B150	PX10	960°C/20 min	40-60	6-15	2%	PX10 masked with UIA
49138	B120	PX10	960°C/20 min	10K	5-10	No P-N Junction	B120 masked with UIA
49147	Dil B150	PX10	960°C/20 min	10-60	10-15	1-11%	PX10 masked with UIA after 400°C bake
50801	B156	PX10	960°C/20 min/N ₂	8-12	8-12	Poor (3%)	PX10 baked in air for 1 hour before dilution
50806	B150	PX10	950°C/20 min/N ₂	10-60	10-15	1%-8%	PX10 masked with UIA
50805	B60	PX10	960°C/20 min/N ₂	50-60	10-15	5%-8%	PX10 masked with UIA; N ⁺ areas on P ⁺ surface
50831	B120	PX10	960°C/20 min/N ₂	some low, 90-100	6-10	Poor (3%)	PX10 and B120 masked with UIA; last 5 min. of diffusion in O ₂
50962	B120	PX10	960°C/20 min/N ₂	10-1000	6-10	Poor (3%)	PX10 and B120 masked with UIA; last 5 min. of diffusion in O ₂

TABLE 3 (Continued)
SIMULTANEOUS DIFFUSION EXPERIMENTS AND RESULTS

Run ID	P ⁺ Dopant	N ⁺ Dopant	Diffusion Conditions	Sheet Resistivity (Ω/□)		Cell Data (Efficiency)	Comments
				p ⁺	N ⁺		
50838	"Diffusol" P	"Diffusol" N	950°C/20 min/N ₂ + O ₂	Unable to strip diffusion glass			
50976	D11 B150	PX10	940°C/20 min/N ₂ - 18 min + O ₂ 5 min	50-200	6-10	0	PX10 masked with X600 experimental SiO ₂
50980	B60	PX10	950°C/20 min/N ₂	-	-	2-5%	PX10 and B60 masked with NP-5R, baked at 400°C
47748	B60	PX10	950°C/20 min/Ar	Generally 8-20 10-40, some 80-120		1-4%	PX10 and B60 masked with NP-5R, baked at 400°C
Dopant Identification							
B10	Allied Chemical Corporation						
B150							
PX10							
NP-5R							
X600							
UIA	Diffusion Technology, Inc.						
B60							
Diffusol "N"	Transene Co.,						
Diffusol "P"	Inc.						

05840:6

Experiment 47748 was diffused in Ar to determine if there was any interaction between the N_2 ambient and the dopant/mask layers which would cause out-diffusion of the dopants.

As seen in Table 3, the maximum cell efficiency obtained in these experiments was 11%; however, the majority of the cells have much lower efficiency (1% - 4%). In all cases when the shunt resistance of the low efficiency cells was measured, it was found to be unacceptably low, generally in the $1-10 \Omega\text{-cm}^2$ range.

After testing, the metal and antireflection coating were removed from a number of cells in the experiments listed in Table 3. These cell blanks had the same sheet resistivity as was measured after diffusion, but a careful point-by-point scan with a conductivity probe showed small N-type areas in the P-type front surface. These areas would be sufficient to produce a short circuit in the cell junction causing the very low shunt resistance and the low IV parameters.

A model was developed to explain the results of these simultaneous diffusion experiments. The phosphorus species diffuse both into the silicon forming the N^+N back junction and outward through the mask. These phosphorus species diffusing through the mask then migrate (in a gas or along the surface of the web) and diffuse into the front surface of the cell. This excess phosphorus in the front surface of the silicon prevents the boron from compensating the web and forming the required P^+N junction. This explanation has been validated by spreading resistance measurements. In some areas on the front surface, the spreading resistance profile is similar to Figure 2, that is, an N^+N junction structure.

In an effort to improve the uniformity of the diffusion mask, an alternative application method was tested. In this technique, the web strip, coated with baked P-type and N-type dopants, was dipped into the SiO_2 solution and slowly withdrawn. This method is completely analogous to the baseline sequence method for applying the antireflective coating. To achieve the proper mask thickness (1500-2000 Å), it was necessary to pull the web from the solution at about 30 cm/min. After baking to remove the solvent, the oxide

layers covering the dopants appeared to be uniform, free of cracks, and crystallization. It was hoped that this SiO_2 layer would form an impermeable diffusion mask.

In the first test, U1A (Diffusion Technology) SiO_2 was used. However as can be seen from data from cells produced in this experiment (Table 4.), the cell efficiencies were very low. Several cells were stripped of metal and antireflective coating and the surfaces mapped with a conductivity probe. On each cell blank, small areas of N-type conductivity were found on the P^+ side front surface. These small areas were apparently sufficient to short out the junction causing the low efficiency. The sheet resistivity was quite variable with values between $5\Omega/\square$ and $300\Omega/\square$. This is a further indication that phosphorus penetrated the front junction since resistivities in the $30\text{--}50\Omega/\square$ are normally obtained.

Very similar results were obtained on the last two experiments indicating that the SiO_2 glasses are not adequate masks.

Based on the data from these experiments, it is obvious that the diffusion masks used were not capable of preventing the out-diffusion of phosphorus and subsequent contamination of the P^+ surface. The problem may be due to the material being used, its method of application, the method of forming the glass, the method of use, or some combination of the above.

The next series of tests investigated various alternative approaches to achieving the simultaneous diffusion while concentrating on the tube type furnace drive process.

2.2.3 Later Approaches

a. Lower Temperature Diffusion

The phase diagram⁽³⁾ of the $\text{SiO}_2\text{--P}_2\text{O}_5$ system shows the P_2O_5 forms a liquid in SiO_2 at temperatures slightly below 1000°C . This suggests the possibility that at 960°C the phosphorus has sufficient mobility to out-diffuse through the mask and onto the front surface. Accordingly,

TABLE 4

SIMULTANEOUS DIFFUSION EXPERIMENTS CONDUCTED WITH DIFFUSION MASKS APPLIED BY DIP COATING

<u>Run No.</u>	<u>P⁺ Dopant</u>	<u>N⁺ Dopant</u>	<u>Diffusion Conditions</u>	<u>Sheet Resistivity (Ω/\square)</u> <u>N_± P_±</u>	<u>Cell Efficiency</u>	<u>Mask</u>
47520	B60	PX10	950°C/20 min 1800 cc/min N ₂	7-9 Variable (5-300)	1-2%	U1A (Dipped) (2000 Å Thick)
50845	B60	PX10	950°C/20 min 1800 cc/min N ₂	10-20 50-200	1-2%	NP-5R (Dipped) (1500 Å Thick)
50846	B60	PX10	950°C/20 min 1800 cc/min N ₂	5-20 50-200	1-3%	NP-5R (Dipped) (2000 Å Thick)

experiments were conducted in which the diffusion temperature was reduced by 100°C to reduce the phosphorus mobility.

The first experiment was conducted using a diffusion temperature of 860°C for 60 minutes. Theoretically, these conditions should produce a back surface field (BSF) of about 0.3 μm and a front junction of 0.15 μm – both significantly more shallow than desired. However, it was felt that the experiment would produce information regarding the mobility of phosphorus. It would also afford an opportunity to determine IV characteristics of a cell with shallow junctions.

A second experiment was then conducted with the diffusion temperature increased slightly to 870°C with the diffusion time held fixed at 60 minutes. In this experiment, the diffusion mask thickness was increased from 1500 Å to 2000 Å to determine if the thicker mask was more impervious to the phosphorus.

After the diffusion step, cell processing was completed using the baseline sequence. The IV properties of the cells were essentially the same as in previous simultaneous diffusion experiments, i.e., low open circuit voltage and low efficiency. All cells had a low shunt resistance of less than 100 Ωcm^2 .

To further analyze the cells, the contact metal and antireflection coating were removed from several cells in each run. The front surface of the cells was mapped with a conductivity probe and showed small areas of N-type material which could act as a shunt leading to the low Voc and low efficiency.

It should be noted that the first low temperature experiment was conducted in a newly cleaned diffusion tube which was tested and found free of contamination. Since the cells produced from this run had similar front surface N-type areas as those in previous simultaneous junction experiments, it was concluded that the source of the noted contamination is not the diffusion tube.

Table 5 summarizes results of the low temperature diffusion experiments along with other experiments described below.

TABLE 5

LOW TEMPERATURE, ARSENIC AND P-TYPE WEB SIMULTANEOUS DIFFUSION EXPERIMENT SUMMARIES

Run ID	Dopants		Diffusion Conditions	Sheet Resistivity (Ω/\square)		Cell Efficiency	Mask	Results
	N ⁺	P ⁺		N ⁺	P ⁺			
50849 (N-base web)	PX-10	B-60	860°C/60 min 1000 cc/min N ₂	20-60	3-60	Low Voc <1%	1500 Å - U1A Dipped 500°C Bake	Low Voc (<20 mV) precluded any efficiency meas.
50850 (N-base web)	PX-10	Dil. B-60 (50/50)	870°C/60 min 1000 cc/min N ₂ 200 cc/min O ₂	20-200	30-300	<1%	2000 Å - U1A Dipped 400°C Bake	Voc slightly higher but poor cells
49252 (N-base web)	As-120	Dil. B-60 (50/50)	950°C/20 min 1000 cc/min N ₂ 180 cc/min O ₂	50-200	Variable 45-250	Max. 3%	1500 Å - U1A Dipped 500°C bake	Max. Voc = 300 mV ⁺ Some strips showed N ⁺ contamination.
49253 (P-base web)	PX-10	B-60	860°C/20 min 1000 cc/min N ₂ 180 cc/min O ₂	60-100	100-300	Mx. 8%	1500 Å - U1A Dipped 400°C Bake	Av Voc = 480 mV ² Av Jsc = 26 mA/cm ² Low FF Efficiency 5-8%

b. Arsenic Diffusion

Arsenic is a much slower diffuser than phosphorus. Therefore, a simultaneous diffusion can be carried out at 950°C-960°C which will give the required P⁺N junction depth of 0.2-0.3 μm. At this temperature, the As doped back N⁺N junction should be 0.3-0.4 μm deep.

For the first experiment with the new doping species, an arsenic doped liquid precursor, AS-120, was used. This material was obtained from Allied Chemical and is an arsenic compound in ethyl alcohol.

The arsenic dopant was applied in the same manner as the PX-10 used in the earlier experiments. After application, it was dried under a heat lamp at 90°C and then baked at 200°C in air for 20 minutes. The SiO₂ diffusion mask was applied over the baked dopant.

Row 3 in Table 5 gives data on the first arsenic experiment together with cell data after baseline processing.

The cells had low efficiencies, and most of the cells had open circuit voltages of less than 100 mV. However, a number of cells had an open circuit voltage above 300 mV and efficiencies of about 3%. All cells showed a low shunt resistance from 40 to 200 Ωcm².

Representative cells from this run were stripped of metal and AR coating. On these cells, also small areas of N⁺ conductivity were found on the P⁺ surface. Thus the As dopant does not significantly improve the cell performance and essentially behaves the same as the phosphorus dopant.

c. Simultaneous Diffusion of P-Type Web

Throughout these experiments, emphasis has been placed on the simultaneous diffusion of N-type web. With N-type web, the back N⁺N junction (doped with fast diffusing phosphorus) can be diffused deep into the web while achieving a shallow front P⁺N junction (doped with slower diffusing boron).

Several experiments were carried out with P-type web. To retain the shallow front junction ($\sim 0.3 \mu\text{m}$), the diffusion was carried out at $\sim 860^\circ\text{C}$ and thus the back junction (boron doped) was extremely shallow resulting in a poorer back surface field. However, it was postulated that by using lower resistivity material, reasonable cell performance could be achieved.

Cell data from one of these runs is included in row 4 of Table 5. As can be seen, the P-base cells exhibited a low average V_{oc} (480 mV) and J_{sc} (26 mA/cm^2). The fill factor varied from 0.40-0.60, and the efficiencies varied from 5% to 8%.

Dark IV measurements were made for two selected P-base, simultaneously diffused cells. These data showed that both cells had excellent shunt resistances - in excess of $100 \text{ k}\Omega\text{cm}^2$. However, the series resistance of the cells was $60 \Omega\text{cm}^2$ and $73 \Omega\text{cm}^2$ respectively. Such a large series resistance would reduce J_{sc} to nearly zero.

To determine if the large measured resistance might be due to a Schottkey barrier on the back surface, a portion of the back metallization was removed and a Ga-In contact applied to several cells. (The Ga-In eutectic alloy is known to make ohmic contact to high resistivity P-type material.) This treatment increased the V_{oc} by 20 mV and increased the efficiency by 1%.

The same effect was noted when the back surface of other cells was damaged by sandblasting. The V_{oc} of the sandblasted cells also increased by 20-30 mV with about a 1% absolute efficiency increase.

Data from P-type cells showed that there was no cross doping under these diffusion conditions employed; however, the boron doped junction was quite shallow and the metallization formed a Schottkey barrier on the back surface. The barrier caused a high series resistance.

2.2.4 Sequential Diffusion of N-Type Web

The major thrust of the program was to show the feasibility of simultaneous diffusion in N-type web. However, it was necessary to establish a baseline

condition, exhibiting that high efficiency cells could be obtained on N-type web using a sequential process. Several such processing runs were made following the diffusion procedure in Table 6. Efficiency data from these cells, also shown in Table 6, indicate that cells can be produced on N-type web with efficiencies comparable to those achieved on P-type web, i.e., average efficiencies greater than 13% when cross contamination is controlled.

2.2.5 Simultaneous Diffusion Using a Belt Furnace

One objective of the program was to show the feasibility of carrying out the simultaneous diffusions in a belt furnace. To accomplish this, a test was made at Radiant Technology Corporation, Cerritos, California, using an IR heated belt furnace in which the diffusion gaseous ambient was controlled to several parts per million. Mr. Paul Alexander, JPL contract monitor, assisted in this test.

For the belt furnace experiment, the web strips were pre-diffusion cleaned at the Westinghouse facility in Pittsburgh, Pennsylvania, and then packed to minimize contamination before the test. At Radiant Technology Corporation, the liquid dopants (Phosphorus, (PX10) and Boron, (B120 and B150) from Allied Chemical Corporation) were applied using a sponge-squeegee. The strips were pre-baked at 200°C after an air dry. The strips were placed on a quartz boat for carrying through the furnace.

The major results of this test were as follows:

1. The proper diffusion temperature (960°C) was obtained for 19 minutes with belt moving at 7 cm/min (slowest speed).
2. Although the cooling rate was faster than desired (46°C/min between 960°C and 720°C), it was determined that this could be adjusted with an additional zone on the furnace.
3. No web strip breakage was noted.

TABLE 6

SEQUENTIAL DIFFUSION OF N-TYPE WEB

1. First Diffusion - Back junction using PX10 with U1A mask on front surface. Diffused at 950°C - 20 min in N₂.
Xj = 0.6 - 0.8 μm
2. Second Diffusion - Front junction using B150 with U1A mask on back surface. Diffused at 950°C/20 min in N₂
Xj = 0.2 - 0.3 μm
3. Cell Efficiency Range - 11.0% - 14.5% on 19.8 cm² cell - 50 cells
4. Average Efficiency - 13.2%

4. The diffusion glasses were stripped after a 30 hour delay during which the diffused strips were returned to Pittsburgh. Some staining was noted on both front and back surfaces of the web strips. Staining was caused by the excessive time lag between diffusion and stripping.
5. Sheet Resistivity Measurements
 - Back surface (PX10 as N^+ dopant) - All strips in $8-12\Omega/\square$ range as desired. All strips N type.
 - Front surface (B120 as P^+ dopant) - About half the strips had low sheet resistivities ($5-10\Omega/\square$) and a mixture of N and P type conductivity. The remainder of the strips had high sheet resistivity ($>1K\Omega/\square$) and had mixed N and P type conductivity.
 - Front (B150 as P^+ dopant) - All strips were in the $45-60\Omega/\square$ range (as desired). They were generally of P-type conductivity with some strips having spots of N-type conductivity.
6. On fabricated cells, the AR coating and plating was generally irregular mainly due to the stains noted above.
7. The cell IV parameters were poor with the maximum cell efficiency being 3%.

After fabrication and testing, the metal was stripped off three cells; and the sheet resistivity and conductivity was mapped on the front and back surfaces.

The back surface of all cells was found to be N-type with a sheet resistivity of $8-12\Omega/\square$ as previously measured. The front surfaces had sheet resistivities generally in the $45-55\Omega/\square$ range, but the surface also showed small areas of N-type conductivity. The sheet resistivity of these small areas was in the $10-20\Omega/\square$ range.

Dark IV and spreading resistance measurements were made on several cells. The cells all had low shunt resistances of less than 5 ohm-cm^2 . Due to this low shunt, the other dark IV parameters such as saturation current and carrier lifetime were not measurable. The spreading resistance data was similar to that shown in Figures 1 and 2.

05510:20

From this belt furnace tests, it has been concluded:

1. A belt furnace can be used to perform simultaneous diffusions and achieve junction depths in the proper range.
2. The same contamination problem encountered in the diffusion furnace experiments and discussed previously in this report is present using a belt furnace for dopant drive.

2.2.6 Conclusions - Simultaneous Diffusions Standard Time/Temperature Cycle

Based on data presented in this section it was obvious that simultaneous diffusion is not feasible using a standard diffusion conditions and the liquid dopants sources. Therefore, during the remainder of the program two new techniques were investigated - laser drive-in and flash diffusion.

2:3 Laser Drive-In for Simultaneous Diffusion

2.3.1 Background

In an attempt to eliminate cross-contamination during simultaneous diffusion, a laser was used to drive the liquid dopants into the dendritic web silicon sheet material. In this technique, the surface of the web is melted (less than 1 μm deep) by a pulsed laser. This local melting should drive in the dopant with minimal opportunity to contaminate the other junction.

2.3.2 Experimental Results, Initial Test

The initial test was carried out at Spectro-Technology in Bellevue, Washington. An excimer laser with a pulse length of 25 nsec and a wavelength of 3080 Å was used. The web was held on a table which was incrementally moved in an x-y motion under the pulsed laser so that the entire surface of the web was treated.

The laser spot size, the table speed, and the table incremental motion were controlled so that varying amounts of power were applied to the surface of the web. Power levels of 1 to 2 J/cm^2 were used.

05510:21

Table 7 lists the experiments carried out. The following general comments can be made:

- Approximately 4 minutes were required to process one side of a 3 cm x 12 cm strip of web.
- Web surfaces were discolored and spotty after the phosphorus drive.
- Web surfaces were quite clean after the boron and aluminum drive.
- The laser lenses had to be cleaned after each phosphorus test to remove "oily" droplets.
- All surfaces showed the effects of the laser heating (footprint of spot) to a greater or lesser degree - generally noted as surface roughness (see Figure 3).
- Due to the number of raster lines/inch, table speed, and rep rate, each portion of the web was heated by the laser 4 times.

The samples were prepared by coating each side of the cleaned web piece (3 cm x 12 cm) with the dopant noted in Table 7. The samples were heated to 400°C for 15 minutes to remove excess solvent and form a doped glass. No diffusion masks were used to cap the doped glass. After drying, the dopant glasses were hard and dry. However, before the laser test, the phosphorus glass (being highly hygroscopic) took on a slightly oily appearance. This is what caused the deposition on the lenses, noted above.

During the laser drive test, the two sides of the web were heated sequentially. However, if this technique were to be used for production, it would be relatively simple to use two lasers to heat the two surfaces of the web simultaneously.

The junction depths of several of the samples were measured using the spreading resistivity technique. Figures 4 and 5 show the front (N^+P) and back (P^+P) junctions for sample 49B which was a P-type web with a phosphorus doped front junction and a boron doped back junction.

TABLE 7

LASER DRIVE IN DIFFUSION TEST

Test No.	Strip ID	Conductivity Type	Experiment (Dopant drive in and emitter or BSF)	Spot Size (mm ²)	Power (J/cm ²)	Lines/in
1	Test Strip	-	---	1	1.1	62
2	49B	P	Phos. drive - emitter	1	1.1	62
3	49A	P	Phos. drive - emitter	1	1.1	62
4	15B	P	Phos. drive - emitter	1	1.1	62
5	17B	P	Phos. drive - emitter	1	1.1	62
6	18A	P	Phos. drive - emitter	1	1.1	62
7	12B	N	Phos. drive - BSF	1	1.1	62
8	63B	N	Phos. drive - BSF	1	1.1	62
9	9A	N	Phos. drive - BSF	1	1.1	62
10	50B	P	Phos. drive - emitter	1	1.1	62
11	14B	P	Phos. drive - emitter	1	1.1	62
12	49B	P	Boron drive - BSF	0.7	2.0	100
13	50B	P	Boron drive - BSF	0.7	2.0	100
14	15B	P	Boron drive - BSF	0.7	2.0	100
15	14B	P	Boron drive - BSF	0.7	2.0	100
16	63B	N	Boron drive - emitter	0.7	2.0	100
17	9A	N	Boron drive - emitter	0.7	2.0	100
18	18A	P	A1 drive - BSF	0.7	1.5	100
19	12B	N	A1 drive - emitter	0.7	1.5	100
20	62B	N	Phos. drive - BSF	0.7	1.5	100
21	49A	P	Boron drive - BSF	1	1.1	62
22	17B	P	Boron drive - BSF	1	1.1	62

05840:18

In all tests, the table speed was 2.5 cm/sec, the rep rate was 50 Hz, and the pulse duration was 25 nsec.



ORIGINAL PAGE IS
OF POOR QUALITY

Sample 17B, P-Base Web, Phosphorus Emitter 1.15 J/cm^2



Sample 17B, P-Base Web, Boron BSF 1.15 J/cm^2

Figure 3. Photomicrographs of Sample 17B Surfaces After Laser Drive of Phosphorus and Boron

n+p FRONT JUNCTION BY LASER DRIVE-IN

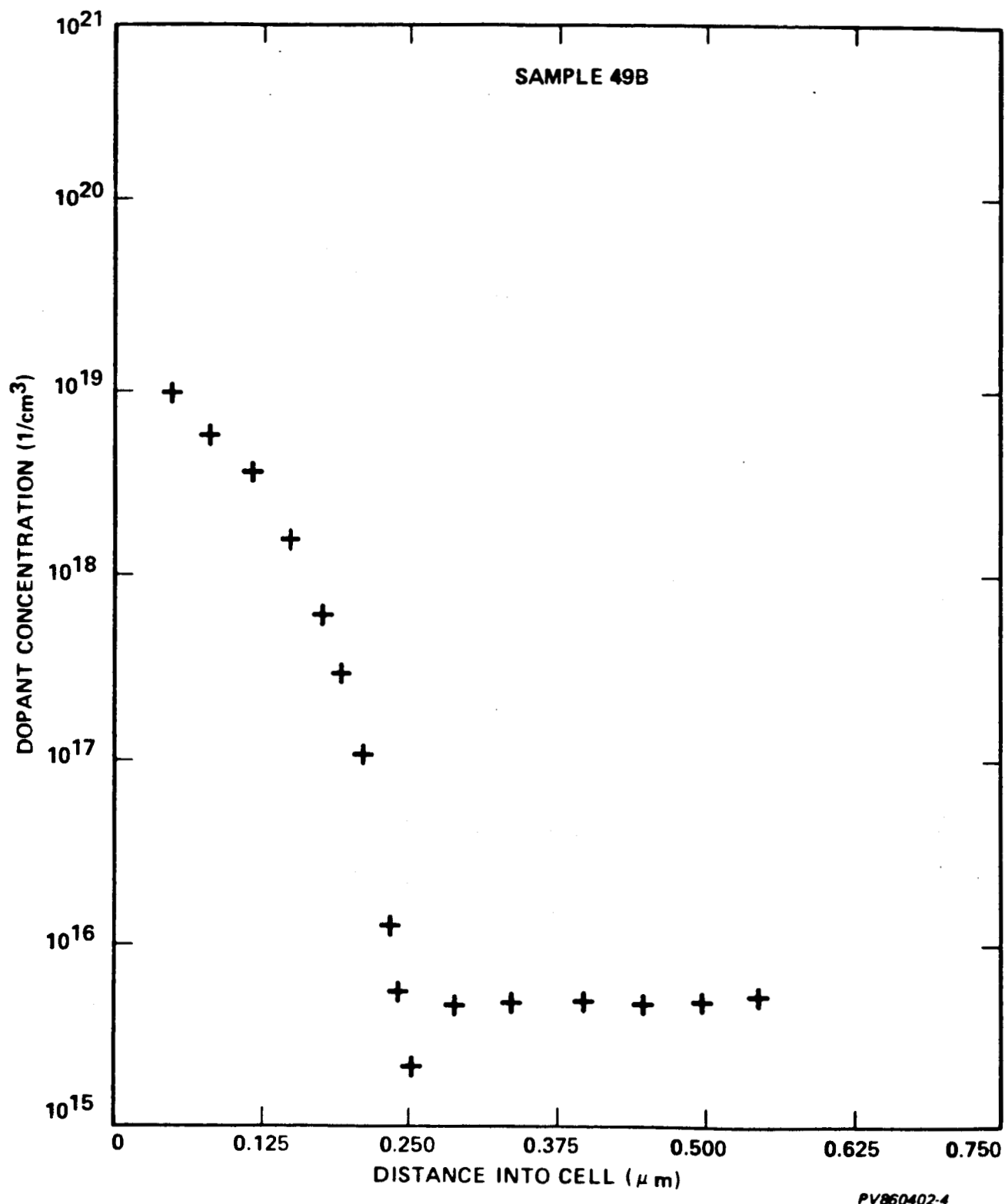


Figure 4. N⁺P Front Junction Profile Measured After Laser Drive on Sample 49B

05840:29

p+p BACK JUNCTION BY LASER DRIVE-IN

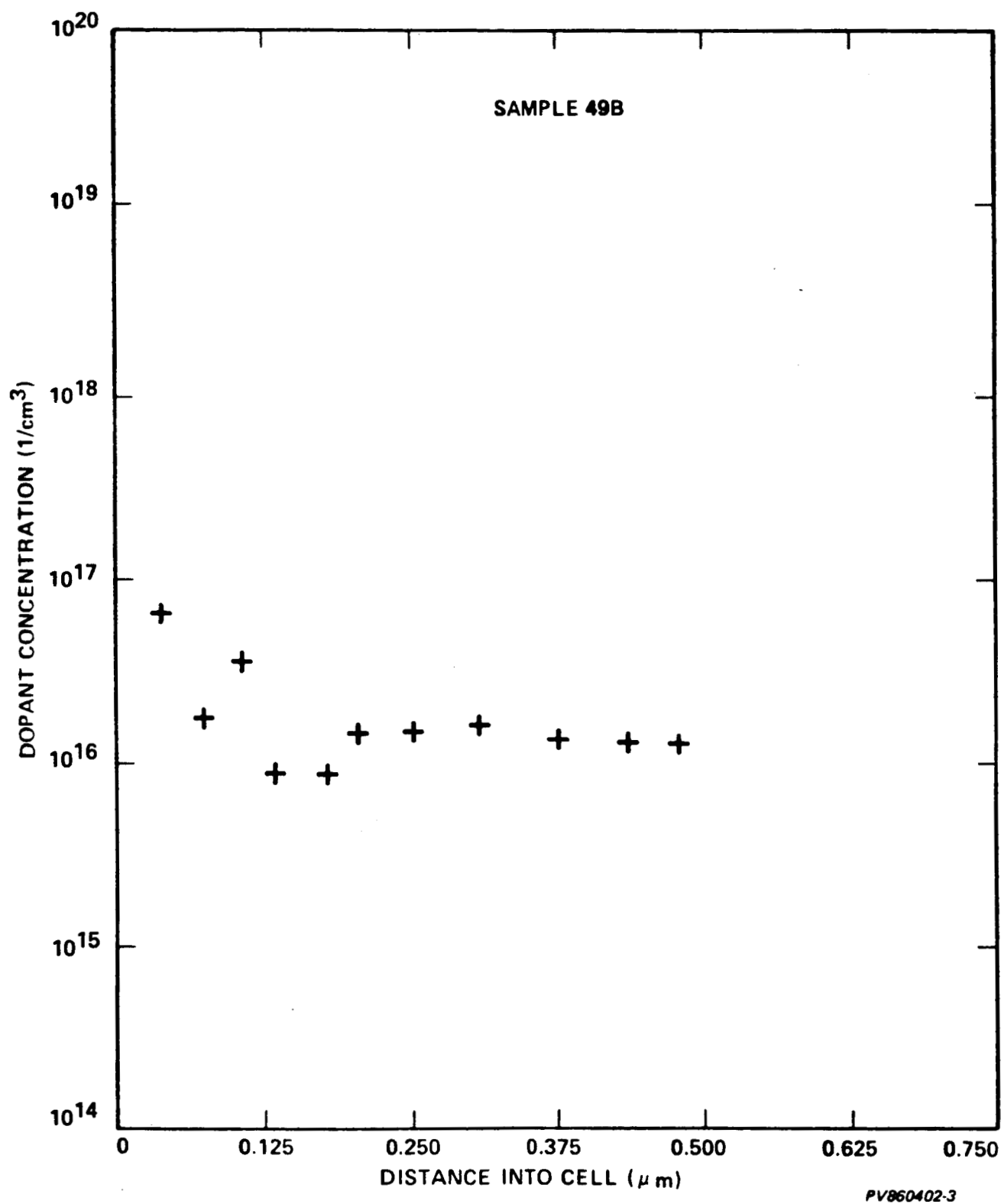


Figure 5. P+P Back Junction Profile Measured After Laser Drive on Sample 49B

05840:30

The front junction with a surface concentration of 10^{19} and 0.25 μm depth is nearly ideal for a solar cell. The low surface concentration will reduce the surface recombination velocity of the carriers without an excessively high sheet resistivity. The data for the P^+ surface indicate a poor back surface junction. From all indications, the boron diffused only slightly into the web with a very low surface concentration.

Six of the samples listed in Table 7 were fabricated into solar cells using the Westinghouse baseline process sequence. Cell data from four of the samples are given in Table 8.

The two P-type cells show the effect of the shallow boron doped back junction. The shallow back surface produces a very high sheet resistivity and a high series resistance. These effects produce the low fill factor and current density seen in the table. In addition, since the back junction is not acting as a back surface field, the open circuit voltage is low, as shown.

The N-type cells also show the effect of the poor boron diffusion. In this case, the emitter junction is not operable, and the cells show essentially no conversion properties.

After the initial cell fabrication test, several additional laser processed samples were heat treated at 800°C for 1 hour in nitrogen and then fabricated into cells. This procedure was carried out in an attempt to relieve any surface stresses. (Any higher temperature processing would tend to drive the dopants further into the crystal.) Table 9 shows IV data from two cells. Conclusions cannot be drawn from only two data points, but there is no obvious improvement in cell quality.

To obtain a control sample, cells from the same web crystals on which the laser processed cells were fabricated, were processed using the Westinghouse baseline process including sequential diffusion of liquid applied boron dopants and liquid applied phosphorus dopants, as well as a liquid applied SiO_2 diffusion mask.

TABLE 8

DATA FROM CELLS FABRICATED USING AN EXCIMER LASER TO FORM THE JUNCTIONS

Cell ID	Web Conductivity Type	Dopants		IV Properties			
		Front	Back	Voc(V)	Jsc $\frac{\text{mA}}{\text{cm}^2}$	FF	$\eta(\%)$
14B	P	P	B	.500	25.4	.66	8.5
50B	P	P	B	.524	24.9	.60	8.0
63B	N	B	P	.080	15.6	.27	0.3
9A	N	B	P	.041	5.2	.33	-

Tested at AM-1, 100 mw/cm^2 , AR coated.

TABLE 9

CELL PROPERTIES MEASURED AFTER HEAT TREATMENT
OF LASER PROCESSED CELLS

<u>Cell ID</u>	<u>Web Conductivity Type</u>	<u>Dopants</u>		<u>IV Properties</u>			
		<u>Front</u>	<u>Back</u>	<u>Voc(V)</u>	<u>Jsc $\frac{\text{mA}}{\text{cm}^2}$</u>	<u>FF</u>	<u>$\eta(\%)$</u>
17B	P	P	B	.317	15.9	.33	1.7
12B	N	Al	P	.002	0.5	----	---

NOTES:

1. Cells annealed at 800°C for 1 hr. in N₂
2. Tested at AM-1, 100 mW/cm², AR coated.

In the control sample test, the six P-base cells had efficiencies between 13.0-14.5% with an average efficiency of 13.6%. The six N-base cells had efficiencies between 12.0% and 13.8% with an average efficiency of 13.5%. These data verify that the web material used in the test was capable of producing high efficiency cells.

In all cells discussed in this section, there was no junction contamination problem noted. That is, none of the phosphorus cross-doped the boron side.

This was checked by conductivity probing the surface of the web.

This initial test indicated that phosphorus can be diffused into dendritic silicon web with a laser power of 1-2 Joules/cm². This phosphorus doped junction is of high quality and suitable for solar cell application. The A1 and B doped junctions, however, were poor and were not suitable as a BSF in P-type material or as an emitter in N-type material.

2.3.3 Subsequent Laser Drive Experimental Results

A subcontract was arranged with Spectro-Technology and a total of three sets of samples were processed. The purpose of these experiments was to study the effects of variations in:

- Laser power
- Spot size
- Type of liquid dopant
- Double laser processing of boron doped side

In these sample sets there were also web pieces with a boron diffused junction for laser processing of a phosphorus doped junction. In addition, parts of the web crystals which were laser processed were also processed using the Westinghouse baseline sequence so it was possible to correlate the parameters of cells produced by the laser drive-in with the baseline process.

Table 10 shows the ranges of the various parameters used in processing these web strips.

TABLE 10

RANGE PARAMETERS - LASER DRIVE IN TESTS

Laser Power (Back)	-	1.0-2.5 J/cm ²	
Laser Power (Back)	-	1.0-2.0 J/cm ²	
Laser Spot Size	-	0.7-1.0 mm	
Dopants (N Type)	-	PX-10	- Allied Chemical Corp.
		P-100	- Allied Chemical Corp.
		Kwik-Kure	- Owens-Illinois Co.
Dopants (P Type)	-	B-150	
		B-60	Allied Chemical Corp.
		A1-10	
Web Conductivity	-	90% P-Type - 10% N-Type	

As in the initial experiments, it was noted that both phosphorus dopants caused problems in that droplets of an oily substance would deposit on the laser lens and reduce the power input to the strip during the processing of the strip. The problem was worst with the PX-10 dopant which is highly hygroscopic but was also noted with the P100.

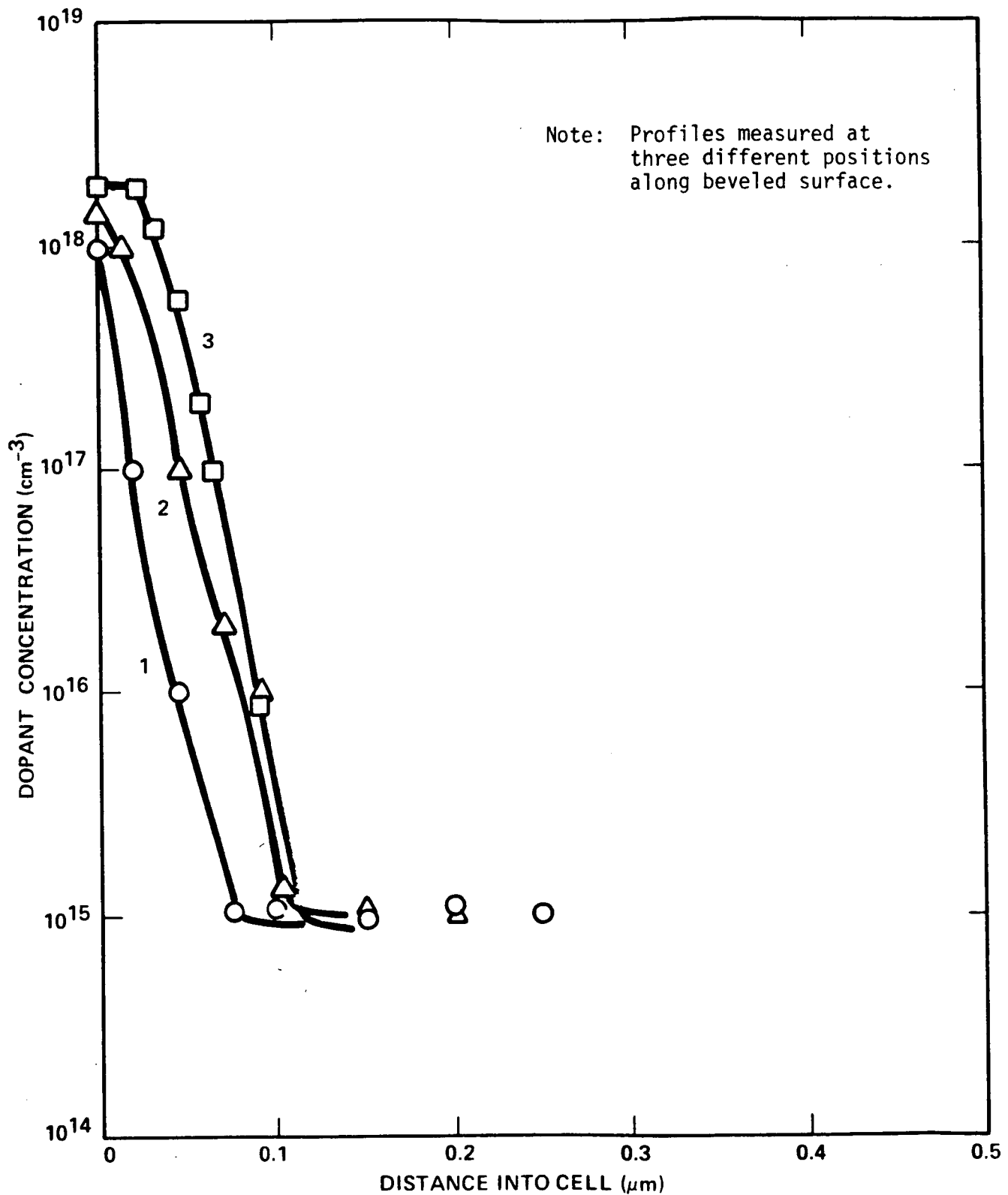
When the samples were returned to AESD for processing, a series of measurements were made including conductivity (both sides), sheet resistivity (both sides) and the front and back junction depth on representative samples.

The sheet resistivities on the laser processed cells, as measured on the back (P^+) surface, were uniformly high, from 300 Ω/\square . (The boron diffused samples had a normal 50 Ω/\square sheet resistivity.) The sheet resistivity did not change with annealing.

The P^+P junction depth was measured on two samples with a back surface dopant source of B150 by spreading resistance. Both a sample annealed at 850°C for 1 hour and an unannealed sample showed essentially no junction with a uniform boron concentration of $1-2 \times 10^{15}$ atoms/cm³. The spreading resistivity trace was taken at three different positions on the beveled surface of the crystal so that different areas of the laser footprint could be scanned. There was no change in the profile with position. The same results were obtained on a sample which had B60 as the back surface dopant source. The samples with the thinner layer of the B150 dopant source and those samples which were processed twice showed the same sheet resistivities as all the other samples processed with the boron back surface dopant.

The sheet resistivity of the front (N^+) surface of the strips was also high, with values ranging from 200 Ω/\square to 1 K Ω/\square . Spreading resistance on a sample which had P100 as the dopant source showed an apparent junction depth of 0.1 μm with a surface concentration of $1-2 \times 10^{18}$ /cm³. As with the back surface, the profile was obtained at three positions along with beveled surface. The profiles were taken about 1.5 mm apart. In this case, the profiles did vary significantly. Figure 6 shows this data. This non-uniformity may be caused by varying thicknesses of the dopant source or inhomogeneities of the laser power. In any case, this non-uniformity would be

SPREADING RESISTANCE PROFILES OF n+p JUNCTION TAKEN 1.5mm APART



PV860402-2

Figure 6. Spreading Resistance Profiles of N⁺P Junction Taken 1.5 mm Apart

05840:31

deleterious to the cell properties. As noted earlier, a somewhat deeper junction depth with a higher surface concentration is desirable for high efficiency cells.

Several strips from Groups 2 and 4 where there was no front surface processing were diffused in a standard phosphorus (POCl_3) process to obtain a diffused N^+P junction coupled with the laser processed P^+P back junction. The sheet resistivities and spreading resistance profile of the front junction of these diffused strips were in the normal range.

After junction drive and after several annealing cycles cells were fabricated on the strips. Lighted IV parameters of selected cells are shown in Table 11. Samples 68-1 and 69-1 had a back diffused junction with a front junction laser processed. These cells had efficiencies nearly equal to the baseline cell, and considerably higher than cells from any other process variation. Cell 51-1 had a POCl_3 diffused junction and a laser driven back junction, and although the efficiency was higher than the totally laser processed cells, it was unacceptably low. The remainder of the cells in which both junctions were laser processed had efficiencies in the 1-8% range. In one case, cell 11-2, there was some improvement due to annealing.

Table 12 shows dark IV data measured on four selected cells. Cell 9-1 had a high series resistance ($2.9 \Omega \text{ cm}^2$) indicating a high sheet resistance from either the emitter or the back surface, or both. The other series resistances were slightly high compared to the normal $0.5 \Omega \text{ cm}^2$. The shunt resistances were all satisfactory although 68-1 at $100 \Omega \text{ cm}^2$ is on the low side.

Cell 12-3 had a high J_{01} of $1.5 \times 10^{-10} \text{ A/cm}^2$ in spite of a reasonable bulk diffusion length. This high J_{01} was probably due to a poor emitter which affects both J_{01} and J_{02} . All of the cells showed high J_{02} which indicate that the N^+P emitter junction is controlling the cell quality.

Cells 9-1 and 11-1 show no beneficial effect from annealings.

TABLE 11

LIGHTED IV PARAMETERS OF REPRESENTATIVE LASER PROCESSED SAMPLES

ID	Dopant		Annealing Treatment	Sheet ρ (Ω/\square)			Conductivity			FF	$\eta(\%)$	Notes
	Front	Back		F	B		F	B	Voc(V)	Jsc $\frac{\text{mA}}{\text{cm}^2}$		
68-1	P100	B150	None	800	22-30		N(P)	P	.545	30.6	.79	13.2 (1, 2)
2.1	P100	B60	Anneal 800°C	130-1K	1K/1K		N(P)	P	No test - Voc	< 0.2 V		
2.3	P100	B60	None	1K/1K	1K/1K		N(P)	P	.414	21.0	.13	1.1 (3)
11-1	P100	B150	Anneal 650°C	200-500	250-300		N(P)	P	.510	24.8	.79	10.1 (3)
11-2	P100	B150	None	200-500	300-350		N(P)	P	.474	22.1	.75	7.9 (3)
9-1	PX10	B150	Anneal 800°C	130-450	380-330		N(P)	P	.494	22.9	.54	6.2 (3)
9-3	PX10	B150	None	1K/1K	260-240		N(P)	P	.402	23.6	.65	6.2 (3)
12-3	P100	B150	None	270-240	230		N(P)	P	.481	22.3	.76	8.1 (1)
69-1	P100	B150	None	---	---		N	P ⁺	.549	30.3	.75	12.5 (5)
51-1	POCl ₃	B150	None	---	---		N	P	.519	25.1	.79	10.4 (3)
56-2	P100	B150	None	---	---		N	P	.448	24.3	.68	7.5 (3)

NOTES: (1) P⁺P junction produced by diffusion.

(2) A cell from the same web crystal fabricated by baseline process had an efficiency of 13.6%.

(3) Slight indication of P type on surface - both junctions laser driven.

(4) All cells were 2.5 cm x 9.8 cm.

(5) POCl₃ front diffused - back laser driven.

05840:21

TABLE 12

DARK IV DATA FROM SELECTED LASER PROCESSED CELLS

<u>Cell ID</u>	<u>Eff. (%)</u>	<u>Rs ($\Omega \text{ cm}^2$)</u>	<u>Rsh ($K \Omega \text{ cm}^2$)</u>	<u>J01 (A/cm^2)</u>	<u>J02 (A/cm^2)</u>	<u>Diffusion Length* (μm)</u>
9-1	6.2	2.9	27	9×10^{-11}	1×10^{-3}	19
11-1	10.1	.68	22	4.7×10^{-11}	1.8×10^{-6}	26
12.3	8.1	.88	6	1.5×10^{-10}	6.4×10^{-6}	19
68-1	13.2	.68	0.1	1.3×10^{-11}	2.5×10^{-4}	36

*Ln measured by surface photovoltage.

TABLE 13
LIGHTED AND DARK IV DATA FROM LASER PROCESSED CELLS
AFTER ANNEALING AND BACK SURFACE DAMAGE

Cell ID	ρ_s (Ω/\square)		Dopants		Laser Power (J/cm ²)	V_{oc} (V)	J_{sc} (mA/cm ²)	FF	EFF (%)	Comments
	F	B	F	B						
34-1	300	700	P100	AL4	2	.432	19.3	.11	1.0	No anneal
34-2	350	1.5K	P100	AL4	2	.373	19.6	.45	3.3	Annealed 1 hr. at 600°C in N ₂
57-1	350	120	P100	B150	2	.497	21.3	.60	6.4	No anneal
57-2	350	130	P100	B150	2	.511	23.8	.78	9.5	Annealed a hr. at 600°C in N ₂
64-1	300	100	P100	B150	2	.511	24.2	.70	8.7	No anneal
64-2	300	100	P100	B150	2	.515	24.4	.73	9.2	Annealed 1 hr. at 600°C in N ₂
42-1	300	600	P100	AL4	2	.494	21.4	.73	7.8	Anneal 700°C 1 hour
42-2	350	1000	P100	AL4	2	.513	25.4	.70	9.2	Damage back and anneal 700°C 1 hour
52-2	260	90	P100	B150	2	.517	24.7	.75	9.6	Anneal 700°C 1 hour
63-2	300	100	P100	B150	2	.527	25.4	.78	10.4	Damage back and anneal 700°C 1 hour

NOTES:

1. AL4 - Allied Chemical - Metallorganic Precursor Containing Aluminum
2. B150 - Allied Chemical - Metallorganic Precursor Containing Boron
3. P100 - Allied Chemical - Metallorganic Precursor Containing Phosphorous
4. All cells AR coated.

Table 13 gives further processing data and lighted IV results from representative cells where the processing included annealing and a back surface damage treatment.

The samples with the Al doped back were poor when no annealing was performed. There was apparently little, if any Al driven into the web crystal as indicated by the high sheet resistivity. This was confirmed by spreading resistance measurements which indicated no appreciable junction.

When these samples were annealed, the characteristics improved somewhat with a maximum efficiency of 7.8% being achieved after a 700°C anneal. When the back surface was damaged by sandblasting before the anneal, the efficiency increased to 9.2%. This is a further indication of a high series resistance associated with the back surface of these cells. The cells with the boron doped back junctions showed somewhat better properties, although the sheet resistance was still high. The maximum efficiency of 9.5% (annealed sample) is more than 4% absolute lower than the efficiency of baseline cells on the same web crystal. The efficiency was also increased on two of the sample cells by annealing at 600°C for 1 hour in N₂. However, both the annealed and unannealed cells had a high series resistance, due to the lack of boron penetration into the crystal.

As in the Al doped samples, the efficiency was further increased to a maximum of 10.4% when the back surface was damaged before annealing.

The conclusion drawn from these data and from previous data is that laser processing as carried out in these tests did not form a suitable back junction. The surface concentrations for the P⁺P junctions are uniformly low. This results in a high series resistance back contact and cells with low efficiency. The front contact, phosphorous doped however, appears to be quite suitable for solar cell application.

This conclusion is confirmed by the dark IV data shown in Table 14. This data is for three of the cells listed previously in Table 13.

TABLE 14

DARK IV DATA FROM FURTHER LASER PROCESSED CELLS

<u>Cell ID</u>	<u>Voc</u> (V)	<u>Jsc</u> (mA/cm ²)	<u>Eff</u> (%)	<u>J01</u> ² A/cm ²	<u>J02</u> (A/cm ²)	<u>Rs</u> (Ω cm ²)	<u>Rsh</u> (Ω cm ²)	<u>Ln</u> (μ m)	<u>Comments</u>
42-1	.494	21.4	7.8	7.1E-11	1.8E-5	1.2	1.8K	30	Anneal 700°C - 1 hr
42-2	.513	25.4	9.2	4.0E-11	1.4E-5	1.4	2.6K	45	Back Damage + 700°C - 1 hr anneal
63-2	.527	25.4	10.4	2.4E-11	2.2E-6	0.6	10.9K	30	Back Damage + 700°C - 1 hr anneal

Diffusion length (Ln) measured by surface photovoltage.

05840:20

The series resistance of Cells 42-1 and 42-1 is high and a resistance of this magnitude would reduce the fill factor and cell efficiency. Cell 63-2 has an acceptable series resistance, but a low efficiency, probably due to an ineffective back surface field.

2.3.4 Conclusion

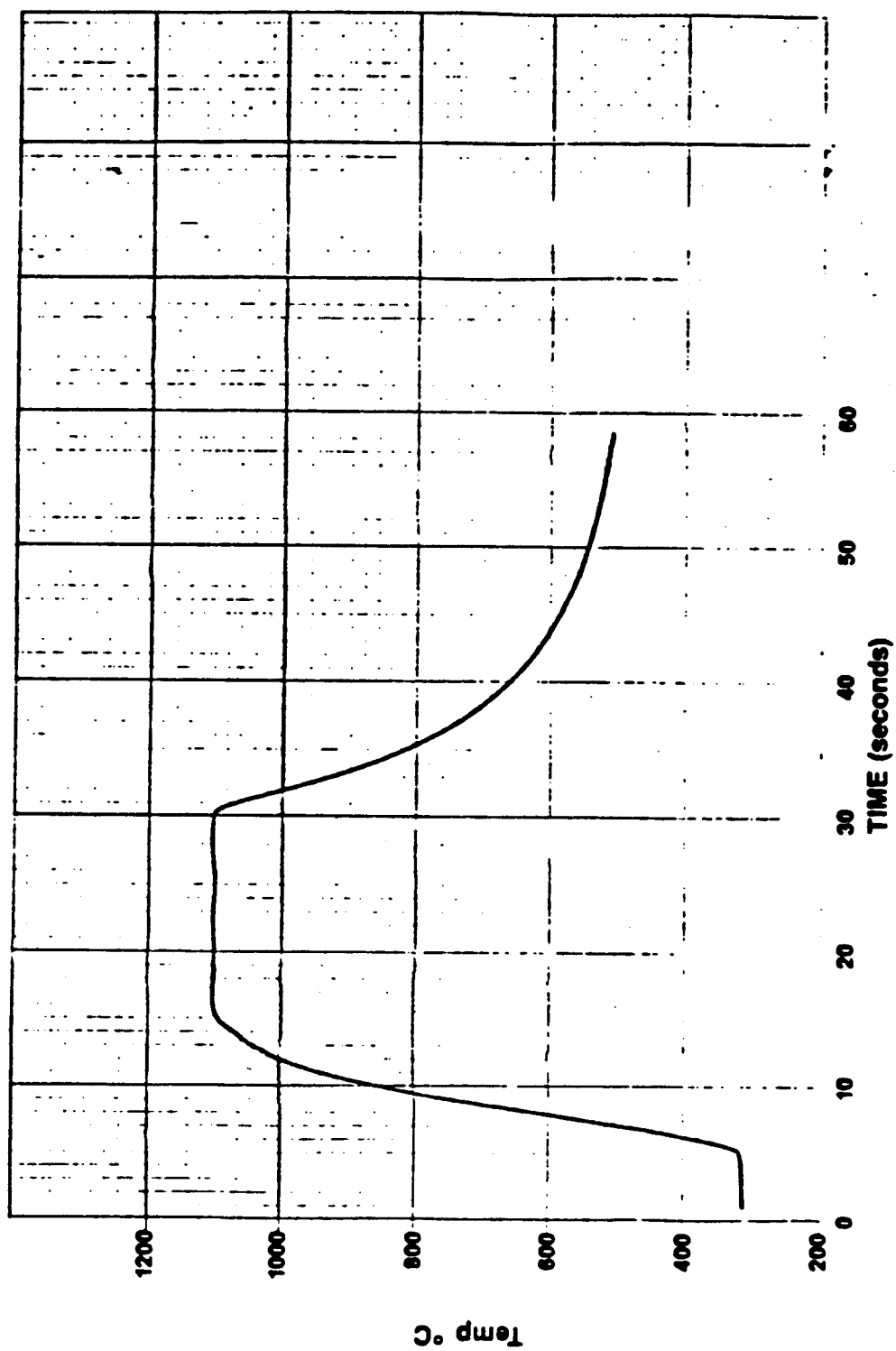
From the excimer laser processing experiments conducted on this program, the following is concluded:

1. There is no cross-contamination of dopants when the front and back junctions are fabricated by laser processing.
2. Both BSF and emitter junctions formed by driving in phosphorus have the depth and surface concentration required for solar cells.
3. Junctions formed by driving either boron or aluminum are extremely shallow ($<0.05\mu\text{m}$) and have a low surface concentration. These junctions are unsuitable for use as either a BSF or an emitter junction.
4. Annealing of the laser fabricated structures improves cell quality slightly, although the maximum values of efficiency obtained are only 60-70% of baseline cell efficiency.
5. Damaging the back surface to assure a low resistance contact increases the laser processed cell efficiency. However, as with annealing the maximum efficiency is still lower than baseline cell efficiency.

2.4 Junction Formation by Pulsed Directed Heating (Flash Diffusion)

2.4.1 Introduction

A novel method of simultaneous junction formation was devised and experiments carried out under Mod-1 and Mod-2 of this contract. In this technique the dopants were applied to both sides of the web strip, dried, and then subjected



AG Associates 1052 Elwell Ct. Palo Alto, CA 94303 415-961-6823

Figure 7. Typical Heating Cycle for Short Time-High Temperature Diffusion

to a short term-high temperature heat pulse to diffuse in both junctions simultaneously. In the studies carried out in this program, the heat pulse was supplied by tungsten-halogen flash lamps. Web material of both P and N-type conductivity of various resistivities was used in these experiments.

Figure 7 shows a typical heat pulse cycle of 1100°C for 15 sec. This curve was supplied by AG Associates, Palo Alto CA, where these experiments were carried out.

There are several distinct advantages to the heat pulse technique. First, the junction formation is rapid, taking less than 1% of the normal time. This reduces processing time and energy costs. Second, both junctions can be diffused simultaneously; and due to the short time period that the Si is at a high temperature, cross-contamination of the dopants should not occur.

2.4.2 Experimental Results

All data reported here was obtained from web strips in which the diffusions were carried out at AG Associates in Palo Alto, CA.

Table 15 shows representative results of conductivity and sheet resistivity measurements on P and N base dendritic web simultaneously diffused using the flash diffusion method. In the case of the P-type material, the sheet resistivity of the front surface (phosphorus doped) is considerably lower than the 60Ω/□ specified for the baseline sequence, while the back sheet resistivity is slightly high. This would be expected since phosphorus diffuses nearly a half an order of magnitude faster than boron at 1100°C.

Figures 8 and 9 show the N⁺P front and P⁺P back junctions for sample #16. The junction depths of 0.15 μm and 0.10μm for the N⁺P front and the P⁺P back junctions are in fair agreement with the depths calculated for a 15 sec. - 1100°C diffusion. The surface concentrations ($7 \times 10^{20}/\text{cm}^3$ for the N⁺ surface and $2 \times 10^{20}/\text{cm}^3$ for the P⁺ surface) are higher than those obtained using the baseline diffusion process. This may be an effect of the very short diffusion time. Somewhat lower concentrations are preferred for high efficiency cells.

TABLE 15

RESULTS OF CONDUCTIVITY AND SHEET RESISTIVITY MEASUREMENTS
MADE ON FLASH DIFFUSED JUNCTIONS

Sample	Conductivity		Sheet Resistivity (Ω/\square)	
	Front	Back	Front	Back
<u>P BASE CELLS</u>				
16	N	P	16	63
19	N	P	24	62
20	N	P	27	80
25	N	P	27	80
<u>N BASE CELLS</u>				
81-1	P	N	60	18
84-2	P	N	55	13
88-1	P	N	50	15

- NOTES: 1. The junctions were diffused simultaneously.
2. There was no evidence of any cross-contamination as measured by conductivity probing.

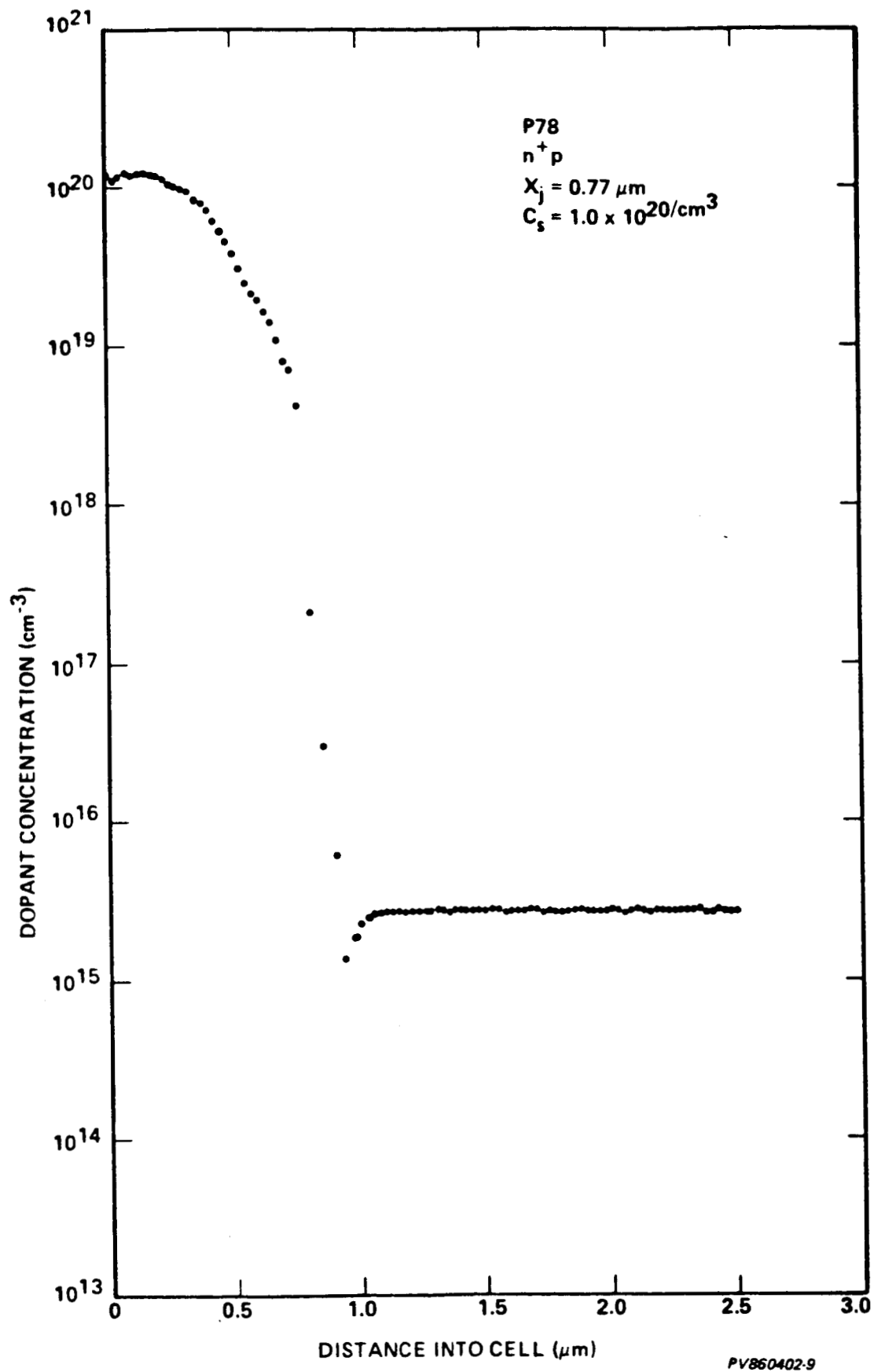
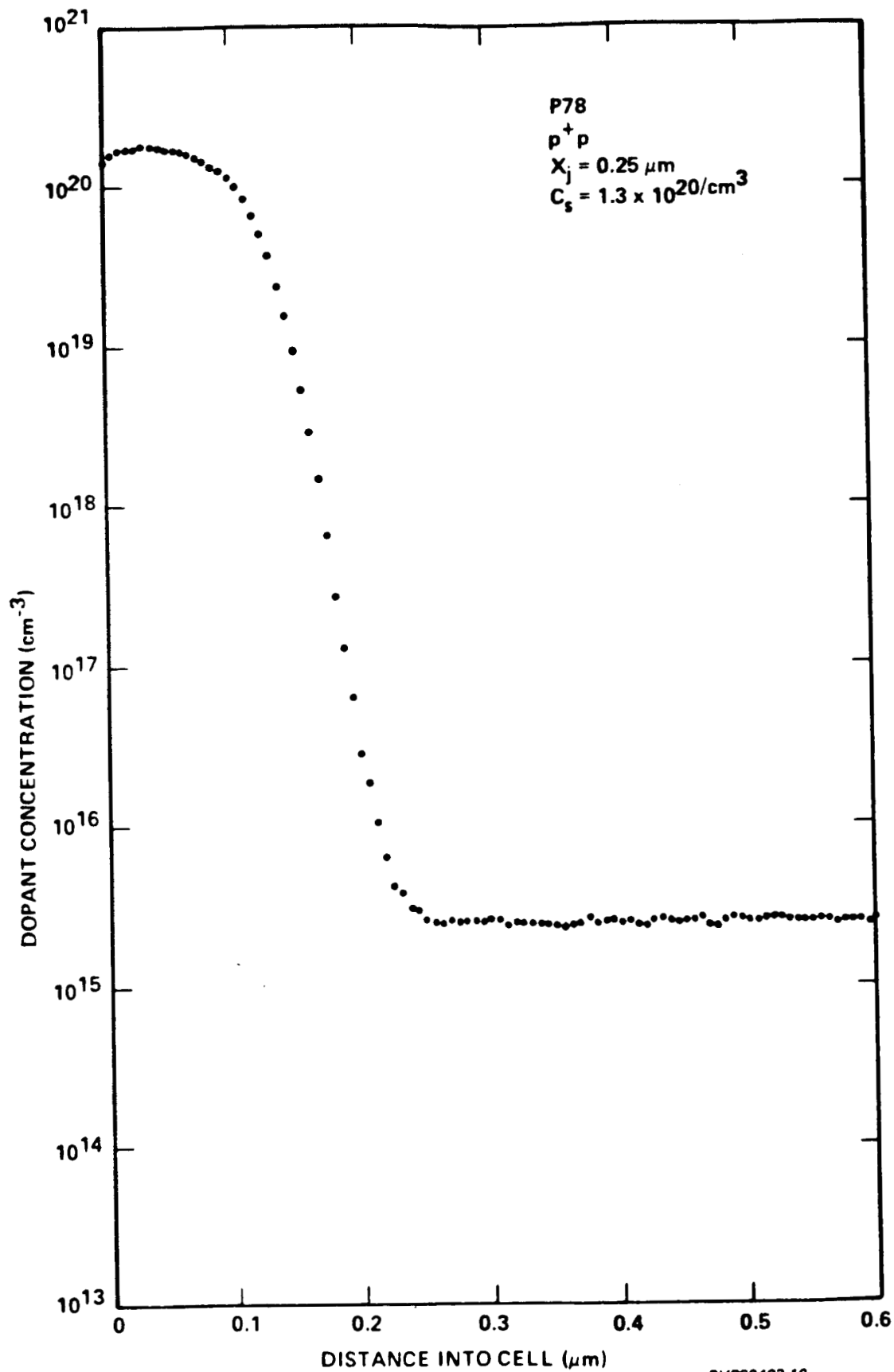


Figure 8. Front N⁺P Junction Formed by Short Time-High Temperature Diffusion
05840:32



PV860402-10

Figure 9. Back P⁺P Junction Formed by Short Time-High Temperature Diffusion
05840:33

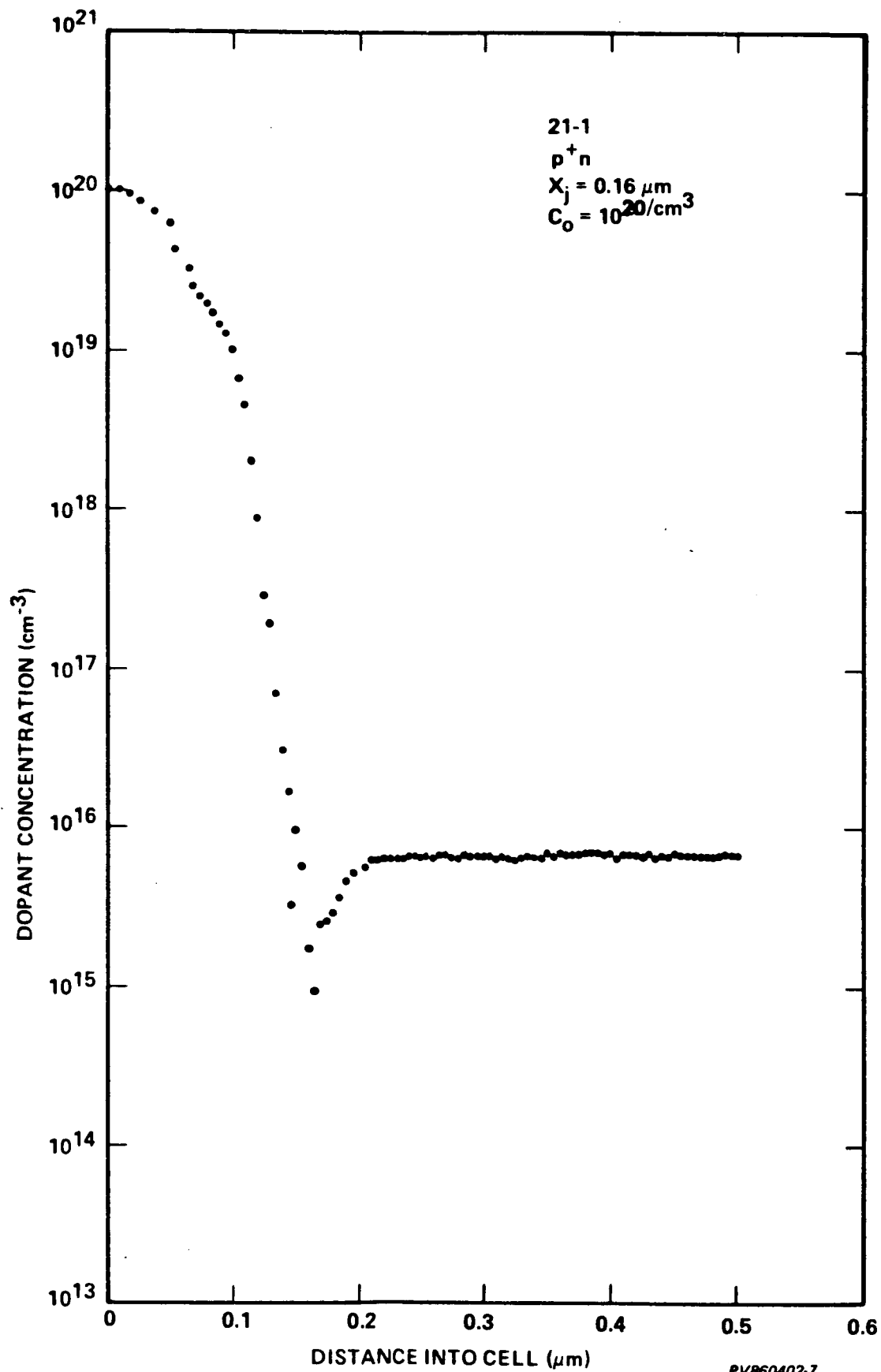


Figure 10. P^+N Front Junction

05840:34

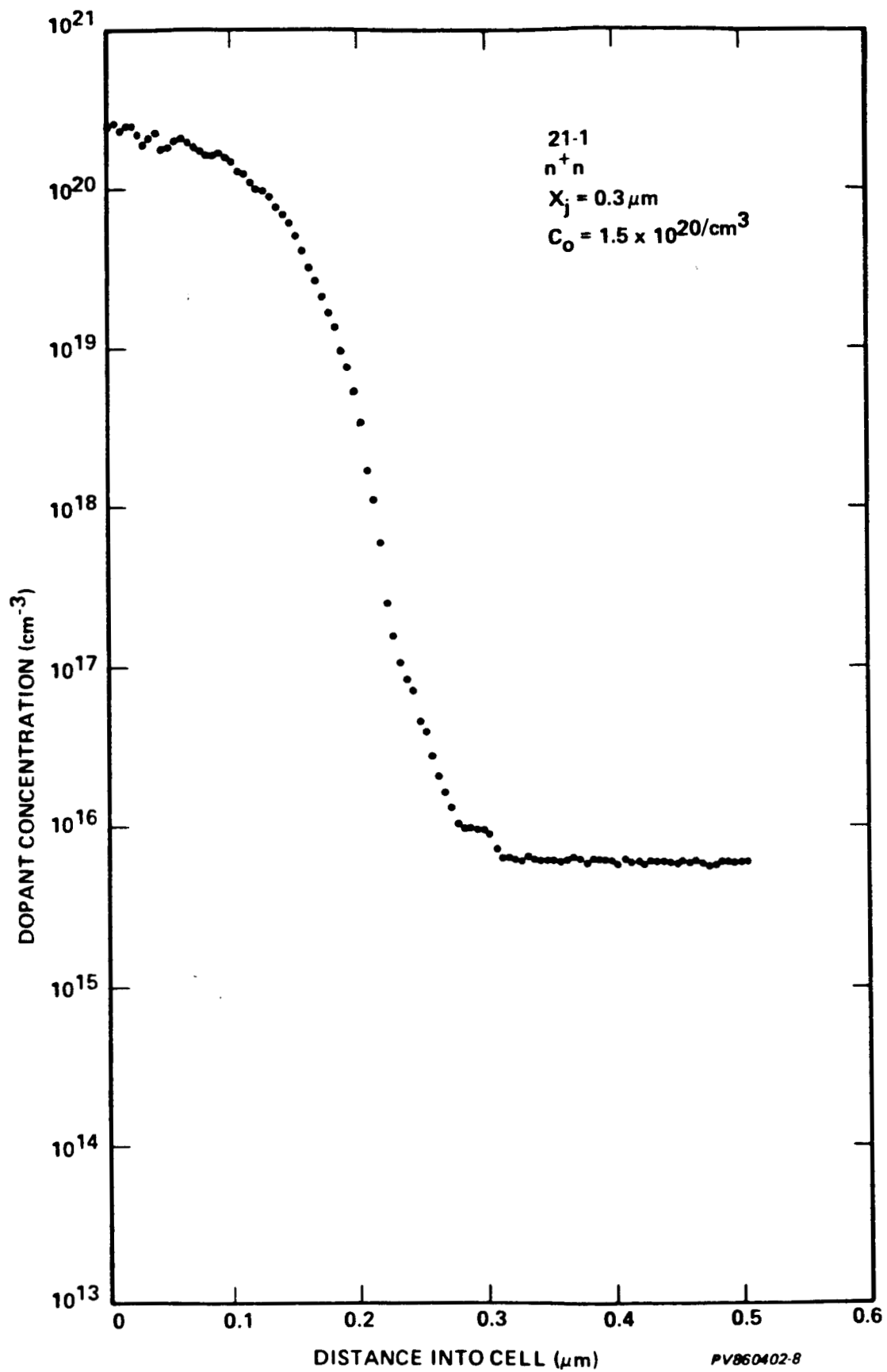


Figure 11. N^+N Back Junction

The sheet resistivity for the N base material is more in line with the baseline sequence specification. The front junction sheet resistivity of $55 \Omega/\square$ is within specifications while the back junction (phosphorus doped) is low ($15 \Omega/\square$ vs $35 \Omega/\square$ specification). However, for a back surface field, this deeper junction should be satisfactory. Figures 10 and 11 show the front P^+N junction profile and the back N^+N junction profile for an N base cell. These junctions are very suitable for solar cells.

Cells were then processed from a number of these initial samples using the Westinghouse baseline sequence. When the cells were fabricated on the as-diffused samples, lower efficiencies were observed than those obtained with the baseline process (diffusion at lower temperatures in a tube furnace).

Rapid cooling from the diffusion temperature (as occurs in the flash diffusion method) will give rise to quenched-in defects. These defects may be vacancy clusters, dislocations, etc., which may or may not be decorated with impurities. However, these defects serve as traps and will reduce the minority carrier diffusion length. These defects or their effects can be partially or wholly removed by various annealing treatments. This annealing may also assure that the dopants are in their proper substitutional lattice sites.

Table 16 gives lighted IV data from a number of cells fabricated on web where the junctions were simultaneously formed by flash diffusion. The table includes data from cells processed with and without annealing after the flash diffusion process.

The data in Table 16 show quite clearly that annealing is required for these samples if a high efficiency cell is to result. The highest efficiency obtained on the unannealed sample was 9.4% for the P base cells and 11.8% for the N base cells. This validates the comments made regarding the quenched in defects due to rapid cooling.

These data show that high efficiency cells can be obtained using this junction formation method with maximum efficiencies of 13.0% for the P base cells and 15.2% for the N base cells.

TABLE 16

LIGHTED IV DATA - CELLS FABRICATED ON WEB WITH JUNCTIONS FORMED
BY PULSED DIRECTED HEATING

<u>Cell ID</u>	<u>Bulk Cond.</u>	<u>Bulk Res.</u> <u>(Ω cm)</u>	<u>Voc</u> <u>(V)</u>	<u>Jsc</u> <u>(mA/cm²)</u>	<u>FF</u>	<u>Eff</u> <u>(%)</u>	<u>Comments</u>
1A	P	4	.065	24.3	.23	1.3	No anneal
1B	P	4	.518	27.1	.75	10.5	900°C - 1 hr
8A	P	4	.497	23.8	.76	9.0	No anneal
8B	P	4	.541	29.1	.78	12.3	800°C - 1 hr
10A	P	4	.537	30.0	.77	12.4	800°C - 1 hr
10B	P	4	.529	26.0	.76	10.5	900°C - 1 hr
12A	P	4	.511	23.6	.78	9.4	No anneal
12B	P	4	.521	27.9	.76	11.0	800°C - 1 hr
61A	P	4	.455	15.8	.77	5.6	No anneal
61B	P	4	.485	17.2	.77	6.4	700°C - 1 hr
66A	P	4	.482	21.0	.47	4.8	800°C - 1/2 hr
66B	P	4	.533	27.3	.77	11.1	900°C - 1/2 hr
49A	P	4	.556	29.3	.79	13.0	850°C - 1/2 hr
49B	P	4	.526	25.5	.75	9.9	700°C - 1 hr
6A	N	1	.556	24.9	.69	9.6	No anneal
6B	N	1	.578	30.5	.75	13.2	800°C - 1 hr
7A	N	1	.561	26.6	.79	11.8	No anneal
7B	N	1	.601	32.9	.77	15.2	800°C - 1 hr
81A	N	1	.560	25.5	.79	11.3	No anneal
81B	N	1	.600	32.2	.78	15.1	800°C - 1 hr
85A	N	0.5	.587	30.5	.79	14.9	700°C - 1 hr
87A	N	1	.583	32.3	.79	14.9	900°C - 1 hr
88A	N	1	.593	32.2	.79	15.0	900°C - 5 min
88B	N	1	.581	29.8	.78	13.5	800°C - 1/2 hr

- NOTES: 1. After annealing samples were cooled at 2-3°C/min.
2. The samples noted as A and B were from the same web crystal.

05840:12

TABLE 17

DARK IV DATA - CELLS FABRICATED ON WEB WITH JUNCTIONS FORMED
BY FLASH DIFFUSION

Cell ID & Treatment	Bulk Cond.	Voc (V)	Jsc (mA/cm ²)	η (%)	R_s (Ω cm ²)	R_{sh} (Ω cm ²)	J_{01} (A/cm ²)	J_{02} (A/cm ²)	L_n (μ m)
8A (no anneal)	P	.497	23.8	9.0	.7	10K	8.7E-11	8.5E-7	30
8B (800°C-1 hr)	P	.541	29.1	12.3	.7	25K	1.4E-11	1.5E-6	48
7A (no anneal)	N	.561	26.6	11.8	.6	2K	6.5E-12	6.0E-6	70
7B(800°C-1 hr)	N	.601	32.9	15.2	.7	.5K	1.5E-12	4.13-5	>200

Diffusion length (L_n) measured by surface photovoltage.

Although further optimization is required, the data in Table 16 show that annealing temperatures approximately 800°C are required. If the annealing is carried out above 800°C, the time must be reduced to prevent further diffusion of the dopant species.

Table 17 shows results of dark IV measurements on four cells with junctions formed by flash diffusion.

These data correlate well with the lighted IV data. Of special note is the greater than 200 μm diffusion length in cell 7B which is about 1.5 that of the total cell thickness.

After the initial feasibility tests a more complete verification experiment was designed and conducted to further investigate the following:

- Conductivity type (P vs N)
- Base resistivity
- Annealing time and temperature

An outline of the experiment is shown in Table 18. A total of 48 strips of each resistivity and conductivity type were diffused yielding a total of 192 samples.

The dopants used were B150 for the boron source and P100 for the phosphorus source. Both sources were obtained from Allied Chemical Corporation. The diffusions were carried out at 1100°C for 10 sec since this cycle had previously produced cells with excellent characteristics.

The annealing cycles used in this test are shown in the first two columns of Table 19. The annealing schedule was set up so that there would be little if any redistribution of the dopants during the heating cycle. Before these annealing cycles were carried out, the diffusion glasses were removed from both sides, thus there was no diffusant source on the web surface during the anneal. In addition, significant diffusion would occur only at the 900°C/30 minute anneal. Therefore, the junction profile should not change during the anneal. This has been verified by spreading resistance measurements.

TABLE 18

FLASH DIFFUSION VERIFICATION EXPERIMENT OUTLINE

	<u>GROWTH RUN</u>
• 48 WEB STRIPS EACH OF: 0.2 Ω cm P TYPE	R499
6 Ω cm P TYPE	R499
	<u>GROWTH RUN</u>
0.2 Ω cm N TYPE	5332
2 Ω cm N TYPE	5332
• RUN R499 - 130 μ m NOMINAL THICKNESS	
RUN 5332 - 100 μ m NOMINAL THICKNESS	
• DIFFUSE AT 1100°C/10 SEC IN ARGON	
• ANNEAL AT TEMPERATURES 900°C to 750°C AND TIME OF 10 MIN. TO 60 MIN. (6 CONDITIONS)	
• COMPLETE BASELINE PROCESS (2.0 x 9.8 CM or 2.5 x 9.8 CM CELLS)	

TABLE 19

FLASH DIFFUSION VERIFICATION EXPERIMENT

ANNEALING (TEMP. °C)	ANNEALING TIME (MIN)	CELL EFFICIENCY (%)			
		N BASE CELLS		P BASE CELLS	
		0.2 - 0.3 Ω CM	2 Ω CM	0.4 - 0.6 Ω CM	6-8 Ω CM
900	30	13.8 (4)	14.2 (2)	11.4 (4)	12.2 (5)
900	10	12.8 (3)	-- (0)	10.4 (4)	11.1 (5)
800	60	13.5 (3)	14.6 (3)	10.8 (5)	11.4 (3)
800	30	14.4 (2)	14.6 (2)	11.4 (5)	11.5 (5)
800	10	14.3 (3)	14.8 (2)	11.0 (6)	11.5 (6)
750	60	14.0 (4)	15.1 (2)	12.1 (6)	11.5 (4)

NOTE: 1) Numbers in parenthesis indicate number of cells tested in each case.
 2) Samples diffused 1100°C/10 sec
 3) Back surface reflector; no passivation

After the annealing cycle, the web strips were processed into cells following the Westinghouse baseline sequence. The cell efficiencies obtained are given in the remaining columns of Table 19. The best overall results were obtained on the 2 Ω cm N base cells where efficiencies greater than 15% were obtained. The P base cells were uniformly lower in efficiency showing no significant improvement in any of the annealing cycles.

The front junction in these P base cells was slightly deeper than on the N base cells ($\sim 0.25\text{ }\mu\text{m}$ vs $0.15\text{ }\mu\text{m}$). However, this is not sufficient to account for the efficiency difference. Conversely, the back junction of the N base cells was deeper than the P base cells. This effect in the P-base cells could result in a less effective back surface field and consequently a lower efficiency cell.

Table 20 gives the diffusion length of selected cells as measured by the SPV technique. The N base cells all had diffusion lengths greater than $125\text{ }\mu\text{m}$ which correlates with the high efficiency cells. The diffusion length of the P base cells is considerably lower, although not sufficiently low to account for the 11-12% cells. No definitive reason for poor performance of the P base cells was developed.

Figure 12 shows the average efficiency of the 2 Ω cm N base cells and 6-8 Ω cm P base cells for various annealing cycle times and temperatures. These data indicate that even higher efficiency N base cells may be obtained with a slightly lower annealing temperature.

Figure 13 shows quantum efficiency curves for an N base and P base cell produced in this experiment. The N base cell (N79) had an efficiency of 15.2% while the P base cell (P77) had an efficiency of 12.2%. This plot indicates the superior red and blue response of the N base cell indicating excellent junction (blue response) and bulk (red response) properties. On the other hand, the curve for the P base cell indicates relatively poor bulk and junction quality. These data are in qualitative agreement with the cell efficiency.

TABLE 20

DIFFUSION LENGTH MEASUREMENTS ON SELECTED FLASH DIFFUSED CELLS

ANNEAL TEMP. (°C)	ANNEAL TIME (MIN)	DIFFUSION LENGTH (mm) BY SPV			
		N TYPE CELLS		P TYPE CELLS	
		0.2 Ω cm	2 Ω cm	0.2 Ω cm	6-8 Ω cm
900	30	--	160	---	50
900	10	125	185	---	25
800	60	--	145	---	92
800	30	--	168	---	75
800	10	--	130	---	75
750	60	--	165	65	---

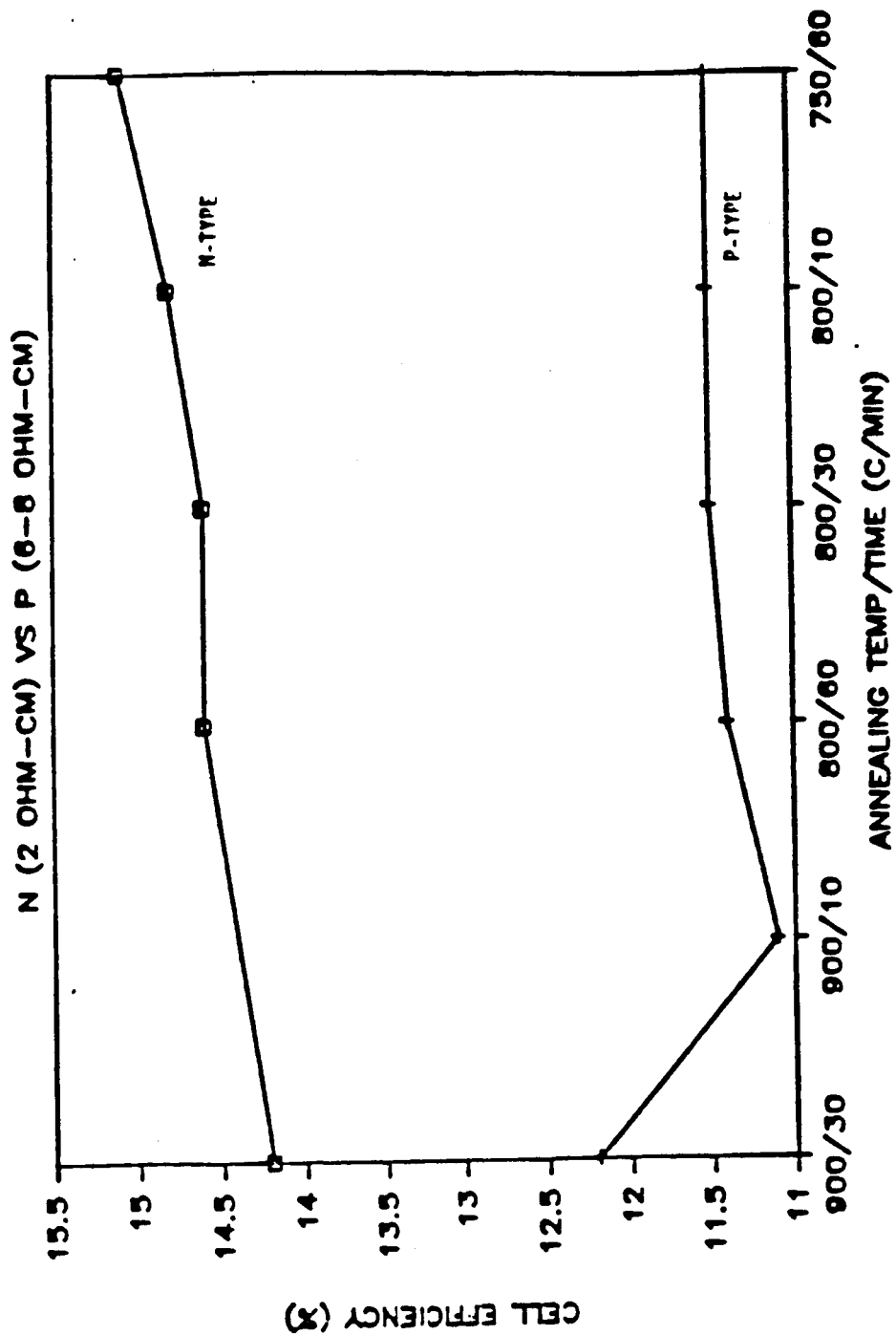


Figure 12. Cell Efficiency vs Annealing Cycle N Base and P Base Cells

05840:37

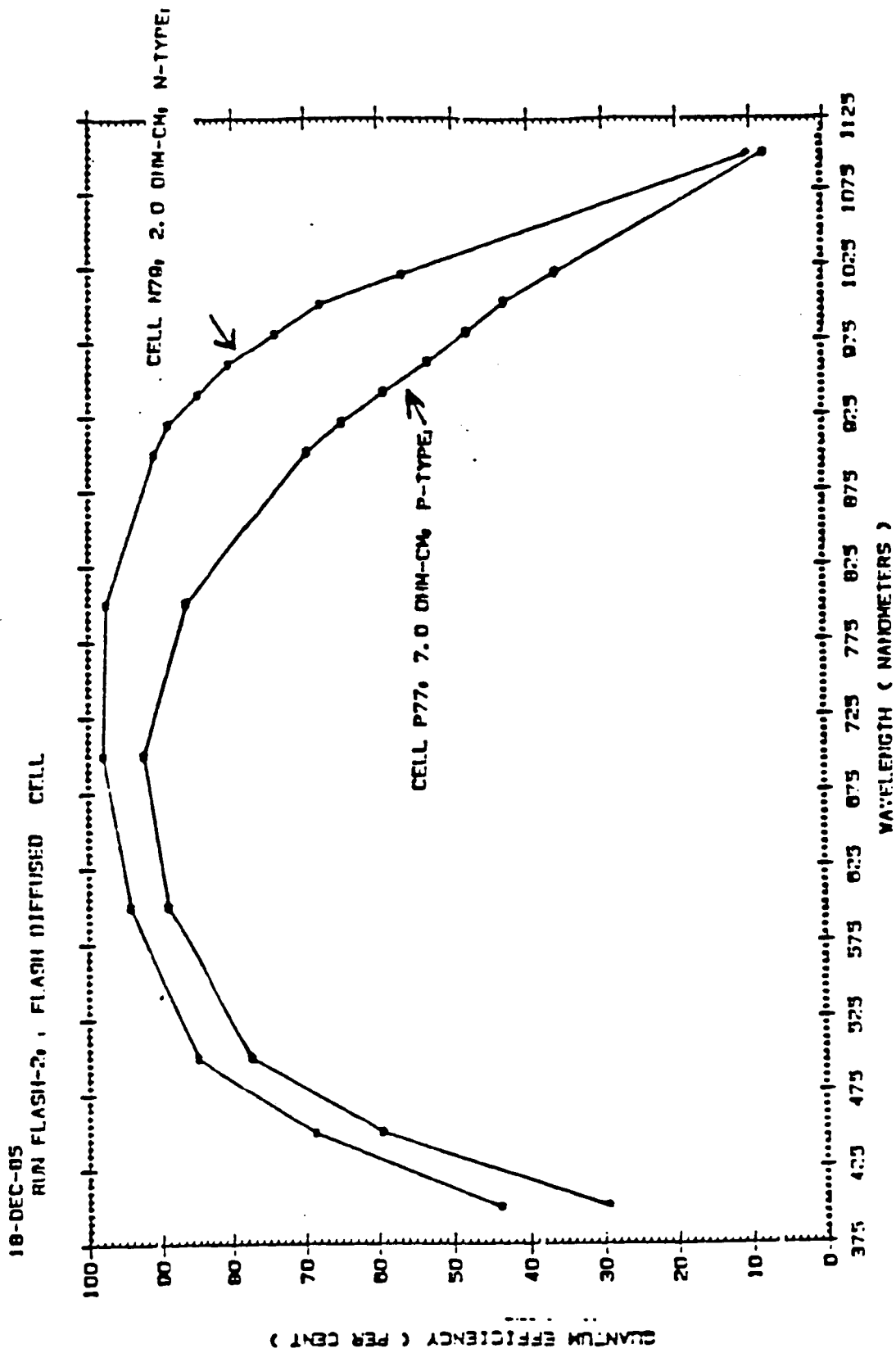


Figure 13. Quantum Efficiency of an N Base Cell and a P Base Cell

05840:38

TABLE 21

COLLECTED DATA FROM FLASH DIFFUSED CELLS

Cell ID	Base Conductivity	Resistivity ($\Omega\text{-cm}$)	Anneal Cycle ($^{\circ}\text{C}/\text{min}$)	EFF (%)	J01 (A/cm^2)	J02 (A/cm^2)	Ln (μm)
7N	N	0.32	900/30	12.5	4.1E-12	2.8E-4	---
10N	N	0.32	900/10	13.1	1.1E-12	1.8E-5	125
47N	N	2.0	900/30	14.2	1.2E-12	2.5E-5	170
58N	N	2.0	800/60	14.9	1.1E-12	2.8E-6	135
65N	N	2.0	800/30	14.7	1.2E-12	1.2E-6	168
79N	N	2.0	750/60	15.2	8.9E-13	7.1E-6	160
48P	P	9.0	900/30	12.5	3.3E-12	4.2E-8	50
57P	P	8.0	800/60	11.8	2.2E-12	9.8E-9	92
71P	P	8.0	800/30	12.2	3.7E-12	2.7E-8	70
77P	P	7.0	800/10	12.2	5.1E-12	6.0E-8	72

Table 21 gives collected data from representative flash diffused cells as a function of annealing time and temperature and conductivity. The bulk material quality for all cells is quite good with J_{01} being in the low 10^{-12} A/cm² range. The junction of the two low resistivity N-type cells are relatively poor. The lower efficiency of cell 7N is apparently due to the junction leakage current.

This data supports the selection of 750-800°C as the preferred annealing temperature.

2.4.3 Conclusions

1. Simultaneous junction formation by flash diffusion is a viable technique to produce high efficiency solar cells
2. N-type web of 2Ωcm resistivity produces the highest efficiency cells.
3. An annealing cycle is required after the diffusion to achieve the highest efficiency.

3.0 COST ANALYSIS

The cost of the simultaneous junction formation step by flash diffusion has been determined using the IPEG formulation. Yearly production rates of 1MW and 25MW were considered so that these costs can be compared to the sequential baseline diffusion process using a tube furnace.

For the 1MW line significant intrastation automation was assumed. For example, when the strips are loaded into cleaning boats, they progress through the cleaning station without any need for operator assistance. Similarly, it was assumed that the meniscus coater applies and dries dopants in one operation after the initial fixture loading. The strips, however, were assumed to be handled manually between the stations. In this process, the operators perform as a team. The throughput of the individual pieces of equipment has been discussed with potential vendors and all are greater than the required 1MW/yr capacity. Therefore, the operators schedule their work to maintain this output by concentrating on specific operations as required. The assumed capital equipment costs include initial engineering.

The 25MW line was assumed to be completely automated. The operators act only as monitors to the equipment and the processes. The capital equipment costs do not include any initial engineering costs. That is, this 25MW/yr facility is a copy of a previously developed line of the same capacity.

The Format A's for the 1 MW/yr and 25 MW/yr facilities are given in Tables 22 and 23 (Two tables are required to define the five operations). All costs are estimated based on present experience and budgetary estimates from potential vendors of equipment and materials. All costs are in 1985 \$. The Format A's for the 25 MW/yr facility are given in Table 24 and 25. Again, costs are in 1985 \$.

The cost of this diffusion step has been determined using the IPEG formula as follows:

$$\text{Cost}\left(\frac{\$}{\text{Watt}}\right) = C_1(\text{Eqpt}) + C_2(\text{Space}) + C_3 (\text{Dir. Labor} + C_4(\text{Matl's} + \text{Utilities}))$$



JET PROPULSION LABORATORY
California Institute of Technology
4800 Oak Grove Dr., Pasadena, CA 91109

TABLE 22 - 1 MW/yr

**SOLAR ARRAY MANUFACTURING INDUSTRY COSTING STANDARDS
FORMAT A - PROCESS DESCRIPTION**

Page 1 of 2

☐ A-1 Process [Referent]

F.L.D.I.F.E.A.N.

Revision Number: 01

Note: Names given in brackets [] are the names of process attributes requested by the SAMIS Computer Program.

☐ A-2 [Descriptive . Name] of process FLASH DIFFUSION PLUS ANNEALING
INCLUDES DOPANT APPL'N AND ETCHING

PART 1 - PRODUCT DESCRIPTION

☐ A-3 [Product . Referent] D.I.F.C.E.L. A-5 Unit of Measure [Product . Units] C.M.2.

☐ A-4 Descriptive Name [Product . Name] D.I.F.F.U.S.E.D. CELL

PART 2 - PROCESS CHARACTERISTICS

☐ A-6 [Output . Rate] (Not Thruput) 174 CM² Units (given on line A-5) Per Operating Minute

☐ A-7 [Inprocess . Inventory . Time] 30 Calendar Minutes

☐ A-8 [Duty . Cycle] 15 Operating Minutes Per Minute

☐ A-8a [Number . Of . Shifts . Per . Day] 3 Shifts

☐ A-8b [Personnel . Integerization . Override . Switch] Off (Off or On)

PART 3 - EQUIPMENT COST FACTORS [Machine . Description]

☐ A-9 Component [Referent] C.L.S.T.A. D.O.P.A.P.P.L. P.U.L.S.E.A.N.N.

☐ A-9a Component [Descriptive . Name] Cleaning station Meniscus Coater Pulse Heating
& drying tunnel for Dopant System
Application

☐ A-10 Base Year for Equipment Prices [Price . Year] 1985 1985 1985

☐ A-11 [Purchase . Cost . Vs . Quantity . Bought . Table] (Number Of and \$ Per Component) 1 120K 1 120K\$ 1 65K

☐ A-12 Anticipated [Useful . Life] (Years) 7 7 7

☐ A-13 [Salvage . Value] (\$ Per Component) 2K 3K 1K

☐ A-14 [Removal . And . Installation . Cost] (\$/Component) 2K 2K 1K

[Payment . Float . Interval] 0.0 0.0 0.0

[Inflation . Rate . Table] IRTJ IRTJ IRTJ

[Equipment . Tax . Depreciation . Method] DDB DDB DDB

[Equipment . Book . Depreciation . Method] SL SL SL



JET PROPULSION LABORATORY
California Institute of Technology
4800 Oak Grove Dr. Pasadena CA 91109

TABLE 23 - 1 MW/yr

SOLAR ARRAY MANUFACTURING INDUSTRY COSTING STANDARDS
FORMAT A - PROCESS DESCRIPTION

Page 2 of 2

☐ A-1 Process [Referent]

Revision Number: _____

Note: Names given in brackets [] are the names of process attributes requested by the SAMIS Computer Program.

☐ A-2 [Descriptive . Name] of process _____

PART 1 - PRODUCT DESCRIPTION

☐ A-3 [Product . Referent] _____

A-5 Unit of Measure [Product . Units] _____

☐ A-4 Descriptive Name [Product . Name] _____

PART 2 - PROCESS CHARACTERISTICS

☐ A-6 [Output . Rate] (Not Thruput) _____ Units (given on line A-5) Per Operating Minute

☐ A-7 [Inprocess . Inventory . Time] _____ Calendar Minutes

☐ A-8 [Duty . Cycle] _____ Operating Minutes Per Minute

☐ A-8a [Number . Of . Shifts . Per . Day] _____ Shifts

☐ A-8b [Personnel . Integerization . Override . Switch] _____ (Off or On)

PART 3 - EQUIPMENT COST FACTORS [Machine . Description]

☐ A-9 Component [Referent] E.T.C.H.S.T.A. B.E.L.T.F.C.E. _____

☐ A-9a Component [Descriptive . Name] Etching Station & drying tunnel Belt Furnace _____

☐ A-10 Base Year for Equipment Prices [Price . Year] 1985 1985 _____

☐ A-11 [Purchase . Cost . Vs . Quantity . Bought . Table] (Number Of and \$ Per Component) 1 75K 1 50K _____

☐ A-12 Anticipated [Useful . Life] (Years) 7 7 _____

☐ A-13 [Salvage . Value] (\$ Per Component) 2K 2K _____

☐ A-14 [Removal . And . Installation . Cost] (\$/Component) 2K 3K _____

[Payment . Float . Interval] 0.0 0.0 0.0

[Inflation . Rate . Table] IRTJ IRTJ IRTJ

[Equipment . Tax . Depreciation . Method] DDB DDB DDB

[Equipment . Book . Depreciation . Method] SL SL SL

A-15 Process Referent (From Front Side Line A-1)

PART 5a - BYPRODUCTS PRODUCED PER MACHINE PER MINUTE [Byproduct]

<input type="checkbox"/> A-20 Catalog Number (Expense Item Referent)	A-22 Amount Produced Per Machine Per Minute [Amount . Per . Cycle]	A-23 Units	A-21 Byproduct Specifications
_____	_____	_____	_____
_____	_____	_____	_____
_____	_____	_____	_____

PART 4 - FLOORSPACE PER MACHINE and PERSONNEL PER MACHINE PER SHIFT [Facility . Or . Personnel Requirement]

<input type="checkbox"/> A-16 Catalog Number (Expense Item Referent)	A-18 Amount Required [Amount . Per . Machine]	A-19 Units	A-17 Requirement Description
A 2 0 6 4 D	200	Sq Ft	Clean Room - Cl. Sta
A 2 0 6 4 D	200	Sq Ft	Clean Room - Pulse Heater
A 2 0 6 4 D	200	Sq Ft	Clean Room - Etch Sta
B 3 6 7 2 D	1.5	PY	Operator Team
A 2 0 6 4 D	300	Sq Ft	Clean Room - Belt Fce
_____	_____	_____	_____
_____	_____	_____	_____

PART 5b - DIRECT REQUIREMENTS PER MACHINE PER MINUTE [Utility . Or . Commodity Requirement]

<input type="checkbox"/> A-20 Catalog Number (Expense Item Referent)	A-22 Amount Required Per Machine Per Minute [Amount . Per . Cycle]	A-23 Units	A-21 Requirement Specifications
E D O P E	1.5E-5	l	Dopants
E 1 3 2 8 D	0.020	Kg	Hydrofluoric Acid
C 1 1 4 4 D	0.01	Cubic M.	D1 H ₂ O
E A C D I D	1.50E-3	Cu M	Acid Bisp
C 1 1 3 2 D	0.025	Kw H	Electricity
E H P E R	2.14E-3	l	Hydrogen Peroxide
E A M H X	6.0E-3	l	Amm. Hydroxide
E 1 3 2 8 D	6.0E-3	l	Hcl
_____	_____	_____	_____
_____	_____	_____	_____
_____	_____	_____	_____

PART 6 - INTRA-INDUSTRY PRODUCT(S) REQUIRED

<input type="checkbox"/> A-24 [Required . Product] (Reference)	A-28 [Yield] (%)	A-26 [Ideal . Ratio] Of Units Out/Units In	A-27 Units of A-26	A-25 Product Name
_____	98	1.00	cm ² /cm ²	Diffused Cell
_____	_____	_____	_____	_____
_____	_____	_____	_____	_____

PREPARED BY R. B. Campbell	COMPANY Westinghouse Electric Corporation	DATE	JPL USE ONLY
CHECKED BY	COMPANY	DATE	<input type="checkbox"/>

REVERSE SIDE JPL 3037-S R 6/81

C1144D - Cost at 2.60 \$/m³
 EDOPE - Cost at 1.50 \$/l
 E1326D - Cost at 1.50 \$/l
 EACDID - Cost at 1.00 \$/Kg

EHPER - Cost at 3.00 \$/l
 EAMHX - Cost at 1.75 \$/l
 E1328D - Cost at 1.60 \$/Kg
 C1132D - Cost at 0.05 \$/Kw
 B36720 - Cost at 16,200 \$/yr unburdened



JET PROPULSION LABORATORY
California Institute of Technology
4800 Oak Grove Dr. Pasadena CA 91106

TABLE 24 - 25 MW/yr

**SOLAR ARRAY MANUFACTURING INDUSTRY COSTING STANDARDS
FORMAT A - PROCESS DESCRIPTION**

Page 1 of 2

☐ A-1 Process [Referent]
F L D I F A N
Revision Number:

Note: Names given in brackets [] are the names of process attributes requested by the SAMIS Computer Program.

☐ A-2 [Descriptive . Name] of process F L A S H , D I F F U S I O N , P L U S , A N N E A L I N G
I N C L U D E S , D O P A N T , A P P L ' N , A N D , E T C H I N G ,

PART 1 - PRODUCT DESCRIPTION

☐ A-3 [Product . Referent] D I F C E L A-5 Unit of Measure [Product . Units] C M 2

☐ A-4 Descriptive Name [Product . Name] D I F F U S E D , C E L L

PART 2 - PROCESS CHARACTERISTICS

☐ A-6 [Output . Rate] (Not Thruput) 4350 CM² Units (given on line A-5) Per Operating Minute

☐ A-7 [Inprocess . Inventory . Time] 30 Calendar Minutes

☐ A-8 [Duty . Cycle] 15 Operating Minutes Per Minute

☐ A-8a [Number . Of . Shifts . Per . Day] 3 Shifts

☐ A-8b [Personnel . Integerization . Override . Switch] Off (Off or On)

PART 3 - EQUIPMENT COST FACTORS [Machine . Description]

☐ A-9 Component [Referent] C L S T A D O P A P P D U L S A N

☐ A-9a Component [Descriptive . Name] Cleaning Station Meniscus Coater Pulse Heating
for Pre-Diff. for Dopant System (Flash
cleaning appl'n Anneal)

☐ A-10 Base Year for Equipment Prices [Price . Year] 1985 1985 1985

☐ A-11 [Purchase . Cost . Vs . Quantity . Bought . Table] (Number Of and \$ Per Component) 1 140,000 1 130,000 5 85,000

☐ A-12 Anticipated [Useful . Life] (Years) 7 7 7

☐ A-13 [Salvage . Value] (\$ Per Component) 2,000 1,000 5,000 A11

☐ A-14 [Removal . And . Installation . Cost] (\$/Component) 3,000 3,000 6,000 5
Units

[Payment . Float . Interval] 0.0 0.0 0.0

[Inflation . Rate . Table] IRTJ IRTJ IRTJ

[Equipment . Tax . Depreciation . Method] DDB DDB DDB

[Equipment . Book . Depreciation . Method] SL SL SL



JET PROPULSION LABORATORY
California Institute of Technology
4800 Oak Grove Dr. Pasadena, CA 91109

SOLAR ARRAY MANUFACTURING INDUSTRY COSTING STANDARDS FORMAT A - PROCESS DESCRIPTION

Page 2 of 2

Note: Names given in brackets [] are the names of process attributes requested by the SAMIS Computer Program.

☐ A-1 Process [Referent]

Revision Number: _____

☐ A-2 [Descriptive . Name] of process _____

PART 1 - PRODUCT DESCRIPTION

☐ A-3 [Product . Referent] _____

A-5 Unit of Measure [Product . Units] _____

☐ A-4 Descriptive Name [Product . Name] _____

PART 2 - PROCESS CHARACTERISTICS

☐ A-6 [Output . Rate] (Not Thruput) _____ Units (given on line A-5) Per Operating Minute

☐ A-7 [Inprocess . Inventory . Time] _____ Calendar Minutes

☐ A-8 [Duty . Cycle] _____ Operating Minutes Per Minute

☐ A-8a [Number . Of . Shifts . Per . Day] _____ Shifts

☐ A-8b [Personnel . Integerization . Override . Switch] _____ (Off or On)

PART 3 - EQUIPMENT COST FACTORS [Machine . Description]

☐ A-9 Component [Referent] E.T.C.H.S.T.A. B.E.L.T.F.C.E.
☐ A-9a Component [Descriptive . Name] Etch Station - Belt furnace
Diffusion Glass for annealing
removal
☐ A-10 Base Year for Equipment Prices [Price . Year] 1985 1985
☐ A-11 [Purchase . Cost . Vs . Quantity . Bought . Table] (Number Of and \$ Per Component) 1 75,000 1 95,000
☐ A-12 Anticipated [Useful . Life] (Years) 7 7
☐ A-13 [Salvage . Value] (\$ Per Component) 2,000 2,000
☐ A-14 [Removal . And . Installation . Cost] (\$/Component) 3,000 3,000
[Payment . Float . Interval] 0.0 0.0 0.0[Inflation . Rate . Table] IRTJ IRTJ IRTJ[Equipment . Tax . Depreciation . Method] DDB DDB DDB[Equipment . Book . Depreciation . Method] SL SL SL

A-15 Process Referent (From Front Side Line A-1) _____

PART 5a - BYPRODUCTS PRODUCED PER MACHINE PER MINUTE [Byproduct]			
<input type="checkbox"/> A-20 Catalog Number (Expense Item Referent)	A-22 Amount Produced Per Machine Per Minute [Amount . Per . Cycle]	A-23 Units	A-21 Byproduct Specifications
_____	_____	_____	_____
_____	_____	_____	_____
_____	_____	_____	_____

PART 4 - FLOORSPACE PER MACHINE and PERSONNEL PER MACHINE PER SHIFT [Facility . Or . Personnel Requirement]			
<input type="checkbox"/> A-16 Catalog Number (Expense Item Referent)	A-18 Amount Required [Amount . Per . Machine]	A-19 Units	A-17 Requirement Description
A, 2, 0, 6, 4, D, _____	400	Sq Ft	Cl. Rm Space - Pre Diff Cl
A, 2, 0, 6, 4, D, _____	800	Sq Ft	Cl. Rm Space - Meniscus Ctr
A, 2, 0, 6, 4, D, _____	600	Sq Ft	Cl. Rm Space - 5 Units - Fl. Diff
A, 2, 0, 6, 4, D, _____	300	Sq Ft	Cl. Rm Space - Etch Sta.
A, 2, 0, 6, 4, D, _____	500	Sq Ft	Cl. Rm Space - Belt Fce
B, 3, 6, 7, 2, D, _____	4	Py	Team Operators
_____	_____	_____	_____
_____	_____	_____	_____

PART 5b - DIRECT REQUIREMENTS PER MACHINE PER MINUTE [Utility . Or . Commodity Requirement]			
<input type="checkbox"/> A-20 Catalog Number (Expense Item Referent)	A-22 Amount Required Per Machine Per Minute [Amount . Per . Cycle]	A-23 Units	A-21 Requirement Specifications
E, A, M, H, X, _____	0.134	l	Ammonium Hydroxide
E, 1, 3, 2, 8, D, _____	0.020	Kg	HF Acid
E, H, C, L, _____	0.130	l	HCL Acid
E, D, O, P, E, _____	3.3×10^{-4}	l	Dopants
E, H, P, E, R, _____	0.055	l ₃	Hydrogen Peroxide
C, 1, 1, 4, 4, D, _____	0.01	M ³	D1 H ₂ O
C, 1, 1, 3, 2, D, _____	0.69	Kw	Electricity
E, A, C, D, I, D, _____	0.06	Gal	Acid Disposal
_____	_____	_____	_____
_____	_____	_____	_____
_____	_____	_____	_____

PART 6 - INTRA-INDUSTRY PRODUCT(S) REQUIRED				
<input type="checkbox"/> A-24 [Required . Product] (Reference)	A-28 [Yield] (%)	A-26 [Ideal . Ratio] Of Units Out/Units In	A-27 Units of A-26	A-25 Product Name
_____	98%	1.00	cm ² /cm ²	Diffused Cell
_____	_____	_____	_____	_____
_____	_____	_____	_____	_____

PREPARED BY _____	COMPANY _____	DATE _____	JPL USE ONLY <input type="checkbox"/>
CHECKED BY _____	COMPANY _____	DATE _____	

REVERSE SIDE JPL 3037-S R 6/81

EAMHX - \$1.75/l
E1328D - \$1.50/Kg
EHCL - \$1.60/l
EDOPE - \$1.50/l
EHPER - \$3.00/l₃
C1144D - \$2.60/M³

C1132D - \$0.05/Kw
EACD1D - \$1.00/Gal
B3672D - Cost at \$16,200/yr unburdened

Where: $C_1 = 0.57$ for 7 yr. depreciation cycle

$$C_2 = \$111$$

$$C_3 = 2.8 \text{ and}$$

$$C_4 = 1.2$$

Table 26 lists the total costs (1985 \$) for the various cost factors in the two line sizes. These figures show significant economy of scale for the large line.

Table 27 shows the results of the IPEG calculations in 1985 \$. To obtain a direct comparison, a similar IPEG calculation was made on the sequential diffusion process.

These data show there is significant cost savings using the flash diffusion process.

In addition, since this process has been shown to produce very high efficiency cells, the potential savings is even greater than shown in Table 27.

TABLE 26

COST FACTORS - 1 MW/YR AND 25 MW/YR FACILITIES
(1985 \$)

	<u>1 MW/YR</u>	<u>25 MW/YR</u>
Capital Equipment	\$295,000	\$531,000
Space (Sq. Ft)	900 Sq. Ft.	2600 Sq. Ft.
Dir. Labor (unburdened)	\$ 97,200	\$259,200
Materials	\$ 26,189	\$384,182
Utilities	\$ 625	\$ 17,147

TABLE 27

COST OF FLASH DIFFUSION VS. SEQUENTIAL DIFFUSION

	<u>1 MW/YR</u>	<u>25 MW/YR</u>
Flash Diffusion (1985\$)	0.57 \$/watt	0.072 \$/watt
Sequential Diffusion (1985\$)	0.92 \$/watt	0.134 \$/watt

4.0 CONCLUSIONS

During this program several different techniques to simultaneously diffuse the front and back junctions in dendritic web silicon were investigated. A successful simultaneous diffusion (as opposed to sequential diffusion) reduces the cost of the solar cells by reducing the number of processing steps, the amount of capital equipment and the labor content.

The three techniques studied were:

1. Simultaneous diffusion at standard temperatures and times using a tube type diffusion furnace or a belt furnace,
2. diffusion using excimer laser drive-in, and
3. Simultaneous diffusion at high temperature and short times using a pulse of high intensity light as the heat source.

The simultaneous diffusion at standard temperatures and times produced front and back junctions which were adequate for solar cell operation; however, in all experiments carried out the fast diffusing phosphorus contaminated the boron doped junction causing diffusion pipes or shorts with a resulting low efficiencies when these samples were processed into cells. The use of various diffusion masks did not prevent this cross-doping.

The use of an excimer laser to drive in the dopants was more successful. There was no cross contamination noted in any of the tests. It was possible to drive in the phosphorus doped junction to the proper junction depth of about 0.18 μm with a low surface concentration. However, under the constraints of the experimental equipment used, an adequate boron doped junction was not achieved. Tests with aluminum as the P type dopant and various annealing cycles did not produce cells with efficiencies greater than 0.65 that of baseline cells. It was concluded that the use of higher laser power should achieve the drive-in of the boron dopant.

The high temperature short time diffusion experiments (flash diffusion) were very successful. When this technique was coupled with a 750-800°C annealing cycles, cells in excess of 15% were produced on N-type material with somewhat lower efficiencies obtained on P-type web. In these experiments an optimum

time and temperature for both the diffusion and annealing cycle were determined.

An IPEG calculation was made to compare the cost of this flash diffusion technique with the baseline sequential diffusion process. Two production quantities were chosen for this comparison: 1 MW/yr and 25 MW/yr facilities.

In both cases there were significant cost savings. In the 1 MW/yr facility the savings was 0.35 \$/watt (~40%) and in the 25 MW/yr facility the savings was 0.062 \$/watt or ~50%.

Acknowledgements

D. L. Meier for dark IV and quantum efficiency measurements and for helpful discussions. K. Tarneja for assistance with liquid dopant studies. A. G. Associates for use of equipment (flash diffusion). A. W. Lilley for help in setting up experimental protocol. E. Dombrowski for assistance in managing program and M. Miller and J. Nydes for technical assistance.

References

- (1) D. L. Flowers and S. Y. Wu, J. Electrochem. Soc., 129, 2299, (1982).
- (2) T. C. Chandler et al, J. Electrochem. Soc., 124, 1409, (1977).
- (3) T. Y. Tein and F. A. Hummel, J. Am. Ceram. Soc., 45 [9] 424, 1962.